A ROBUST DECISION-MAKING TECHNIQUE FOR WATER MANAGEMENT UNDER DECADAL SCALE CLIMATE VARIABILITY

By

LOGAN M. CALLIHAN

B.A., Trinity University, 2009

A thesis submitted to the

faculty of the Graduate School of the

University of Colorado in partial fulfillment

of the requirements for the degree of

Master of Science

Department of Civil, Environmental, and Architectural Engineering

2013

This thesis entitled:

A Robust Decision-Making Technique for Water Management Under Decadal Scale Climate Variability

written by Logan M. Callihan

has been approved for the Department of Civil, Environmental and Architectural Engineering

_____

Edith Zagona

_____

Balaji Rajagopalan

Date_____

The final copy of this thesis has been examined by the signatories, and we

find that both the content and the form meet acceptable presentation standards

of scholarly work in the above mentioned discipline.

Logan M. Callihan (M.S., Civil, Environmental, and Architectural Engineering)

A Robust Decision-Making Technique for Water Management Under Decadal Scale Climate Variability

Thesis directed by Professor Edith Zagona

Previous approaches to water resources planning under inter-annual climate variability combining skillful seasonal flow forecasts with climatology for subsequent years are not skillful for medium term (i.e. decadal scale) projections as decision makers are not able to plan adequately to avoid vulnerabilities. This research addresses this need by integrating skillful decadal scale streamflow projections into the robust decision making framework and making the probability distribution of this projection available to the decision making logic. The range of possible future hydrologic scenarios can be defined using a variety of nonparametric methods. Once defined, an ensemble projection of decadal flow scenarios is generated from a wavelet-based spectral K-nearest-neighbor resampling approach using historical and paleo-reconstructed data. This method has been shown to generate skillful medium term projections with a rich variety of natural variability. The current state of the system in combination with the probability distribution of the projected flow ensembles enables the selection of appropriate decision options. This process is repeated for each year of the planning horizon—resulting in system outcomes that can be evaluated on their performance and resiliency.

The research utilizes the RiverSMART suite of software modeling and analysis tools developed under the Bureau of Reclamation's WaterSMART initiative and built around the RiverWare modeling environment. A case study is developed for the Gunnison and Upper Colorado River Basins demonstrates the utility of the decision-making framework.

ACKNOWLEDGEMENTS

TABLE OF CONTENTS

LIST OF TABLES

LIST OF FIGURES

CHAPTER 1: INTRODUCTION

Water managers and decision makers alike are continuously confronted with the challenges of climate variability and change, and faced with the uncertainty intrinsic to understanding future climate conditions. As variations and changes in climate impact the type and quantity of precipitation, the timing of runoff, evaporation rates, water supply reliability, demands and the occurrence of extreme hydrologic events, the associated uncertainties have far-reaching implications on water resources planning and management. The challenges of planning under climate change are further exacerbated by how current decision-making paradigms incorporate climate change information and deal with the associated uncertainty.

Under traditional "top down" planning approaches, the effects of climate change on streamflow are projected using output from general circulation models (GCMs), which assume future levels of greenhouse gases (GHG) and compute a coarse global, three dimensional grid of raw climate variables. To make the raw global climate variables relevant to regional spatial scales, GCM projections must be bias corrected and "down-scaled" using statistical methods and finer resolution regional climate models [*Hidalgo et al*., 2008*; Tebaldi et al*., 2005; *Wood et al*., 2004]. Once this is accomplished, the downscaled and bias-corrected climate variables may be used as input into hydrologic models, ultimately resulting in regional streamflow projections. The streamflow projections can then be input into water management models to assess the impacts of climate change.

In light of climate change, the use of top-down planning approaches has become irrelevant as the decision-making process relies on the quantification of risk—which proves challenging when the uncertainties associated with climate change remain unknown. Furthermore, the use of GCM projections to inform water management decisions remains

controversial because of significant uncertainties associated with future GHG levels, bias corrections, downscaling, and model congruity. Additionally, because top-down approaches use GCM projections as a starting point, the associated uncertainties propagate throughout an entire study, proving difficult for decision makers to effectively utilize the results [*Weaver et al.*, 2013; *Brown et al.*, 2010; *Wilby and Desai*, 2010; *Hallegatte*, 2009; *Stainforth et al.*, 2007]. Further, like all models, GCM models are based on assumptions that inherently limit the range of results and, consequently, underestimate the full range of future climate outcomes [*Hallegatte*, 2009]. This limitation greatly impacts the decision-making process as decision-makers are forced to make decisions based on joint probability distributions representing the range of possible future climate outcomes [*Lempert and Groves*, 2010].

In an effort to better incorporate climate change uncertainty, bottom-up approaches are becoming increasingly prevalent. In contrast to top-down approaches, the bottom-up approaches begin at the decision-making level and aim to link system vulnerabilities and risk to climate [*Brown et al.*, 2012; *Wilby and Desai*, 2010; *Desai et al.*, 2009]. Typically, historical records are used to understand how the system behaves under certain climate conditions and, given this understanding, decision-makers can identify climate conditions that push the system into vulnerable states under a proposed set of management strategies [*Weaver et al.*, 2013; *Brown et al.*, 2012; *Wilby and Desai*, 2010]. System vulnerability is commonly quantified using system performance metrics and thresholds that, when violated, signify the need for improved resource management. These thresholds are often developed through stakeholder collaboration and must be established before the decision-making process can progress. Examples of such system performance metrics include minimum fish flows, hydropower generation, water shortages, and maximum channel capacity for flood control [*U.S. Bureau of Reclamation*, 2012].

A fundamental concept of bottom-up approaches is the idea of robustness. Unlike top-down approaches—which focus on choosing optimal management strategies based on best estimates of future probability distributions—bottom-up approaches incorporate a robustness criterion [*Lempert and Groves*, 2010]. While there are many different working definitions of robustness, robust decisions generally perform reasonably well over a wide range of plausible future conditions. The integration of robustness tests a decision's ability to perform over a wide range of plausible future conditions—which cannot be quantified using probability theory [*Brown et al.*, 2012; *Lempert et al*., 2006]. Previous literature notes that system performance is often compromised with more robust strategies, while regret under particular future outcomes is minimized [*Weaver et al.*, 2013].

Due to their inherent nature, conventional bottom-up frameworks fail to incorporate regional climate information derived from GCM projections. *Brown et al.* [2012] attempted to ameliorate this deficiency by developing a decision scaling framework that links bottom-up analysis with the use of top-down GCM projections. In this hybrid framework, bottom-up approaches are utilized to identify climate conditions relevant to the decision space, which are then linked to climate information derived from GCM projections. The inclusion of the GCM climate information helps decision-makers differentiate preferences among various management strategies. For more in-depth information on this hybrid approach, the reader is referred to *Brown et al*. [2012].

While the *Brown et al.* framework is a crucial first step, decision-makers must also have access to the climate-variable information that is used to derive associated streamflow projections. Without this important data, decision-makers cannot effectively link management strategies to specific climate variables (i.e., temperature and precipitation). By understanding the

relationship between climate change and system performance, this research demonstrates that decision-makers can implement more flexible and dynamic management strategies that respond to changing climates. This approach differs from traditional engineering approaches that focus on long-term infrastructure options (e.g., reuse, water importation and new storage)—which cannot easily adapt to climate change.

While it is essential that decision-making frameworks incorporate credible information from GCM projections, it is equally important that they consider the impacts of natural variability. For example, in the Colorado River Basin, the mean flow for a 10 year moving window can vary from 82% (12.4 MAF) to 126% (18.9 MAF) of the full record mean [*Nowak et al.,* 2011]. Over a decadal horizon, these variations will likely have an equal, if not larger, impact on system reliability and performance compared to slower moving, anthropogenic-induced climate change trends [*Nowak et al.,* 2011**;** *Solomon et al*., 2011].

Further, recent research links multi-decadal variability in the Colorado River Basin to larger scale climate indicators such as the Pacific Decadal Oscillation and the Atlantic Multi-Decadal Oscillation [*Nowak et al*., 2012]. Unfortunately, the GCMs developed thus far do not model these process which have been identified as drivers of hydroclimatic variability *[Nowak et al.*, 2012; *Timilsena et al.*, 2009; *McCabe et al.*, 2007; *Hidalgo and Dracup*, 2003; *Cayan et al.*, 1999; *McCabe and Dettinger*, 1999; *Piechota et al.*, 1997]. Utilizing projections that incorporate teleconnections with decadal scale signals could improve decision-making and aid in more flexible and dynamic management, as decision-makers will have the tools to better understand how large scale climate indicators may directly impact hydroclimatic variability and management strategies.

The importance of natural variability—including the known impact of decadal and mutli-decadal scale climate indicators on hydroclimatic variability—in the Colorado River Basin highlights the need for projections that incorporate information on decadal timescales. While the utility for using decadal scale projections has been widely recognized by the climate community, research for creating and incorporating decadal scale projections is in its nascent phase [*Solomon et al.*, 2011*; Mehta et al.*, 2011*; Meehl et al.*, 2009*; Keenlyside et al.*, 2008].

Given the existing tools for robust decision-making and an increased understanding of the importance of both climate change and natural variability, our research proposes a novel framework that incorporates decadal scale projections to inform the decision-making process. Similar to *Brown et al.* [2012], this framework is a hybrid approach that capitalizes on the strengths of both "top-down" and "bottom-up" frameworks. We first introduce the methodology for developing decadal scale projections that utilize teleconnections and describe the methodology for applying these projections in a robust decision-making framework on the Upper Colorado and Gunnison River Basins. Lastly we present our results, and a discussion of the research implications.

CHAPTER 2: DECADAL SCALE PROJECTIONS

This chapter develops and demonstrates a methodology for creating decadal scale projections using quasi-periodic features which have been linked to large scale climate indicators. The goal of the projection methodology is to characterize natural variability cycles at any timestep, and based on that create projections that can be used to inform the decision-making process (Chapter 3). In essence, these projections project future variability based on knowledge of current variability cycles. Our methodology expands on two existing frameworks: the Wavelet Auto Regressive Method and the Enhanced Wavelet Auto Regressive Method, briefly discussed below. The introduction of these frameworks is followed by the motivation for developing our methodology, a description of our methodology, the application of the methodology to streamflow data at Lees Ferry, AZ, and lastly, a summary of results, conclusions and directions for future work.

2.1 Overview of the WARM Framework

To explore alternative options for modeling and simulating quasi-periodic time series data, Kwon *et al.* developed a Wavelet Auto Regressive Method (WARM) framework that combines autoregressive modeling with wavelet decomposition. In this framework, a continuous wavelet transform is used to decompose a time series (x_t) into statistically significant periodic components, which can then be simulated using linear autoregressive (AR) time series models, hence the name WARM. The wavelet transform is defined as:

$$X(a, b) = |a|^{-1/2} \int_{-\infty}^{+\infty} x_t \varphi^* \left(\frac{t-b}{a} \right) dt \quad \textbf{Equation 1}$$

where *a* is a scale parameter, *b* is the shift parameter and φ^* is the complex conjugate wavelet function that satisfies specific mathematical properties [*Torrence and Compo*, 1998]. By varying the scale and shift parameters, the wavelet function transforms the decomposed time series data in both time and space [*Torrence and Compo*, 1998]. For the purpose of WARM framework, the Morlet wavelet function was applied:

$$\varphi[\eta] = \pi^{-\frac{1}{4}} e^{i\omega_0 \eta} e^{\frac{-\eta^2}{2}} \quad \textbf{Equation 2}$$

In Equation 2, ω_0 equals 6, is a non-dimensional frequency domain and η is a non-dimensional time domain [*Torrence and Compo*, 1998]. Additional details describing wavelet analysis coupled with the derivation of Equations 1 and Equation 2 can be found in *Torrence and Compo* [1998].

Equations 1 and 2 were applied to the historical streamflow data at Lees Ferry, AZ (1906-2005); the results are illustrated in Figure 1C.
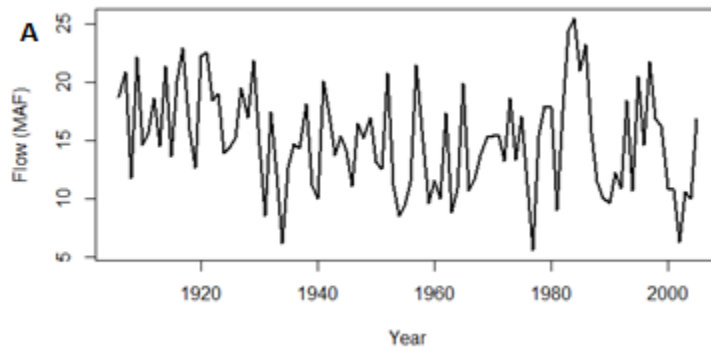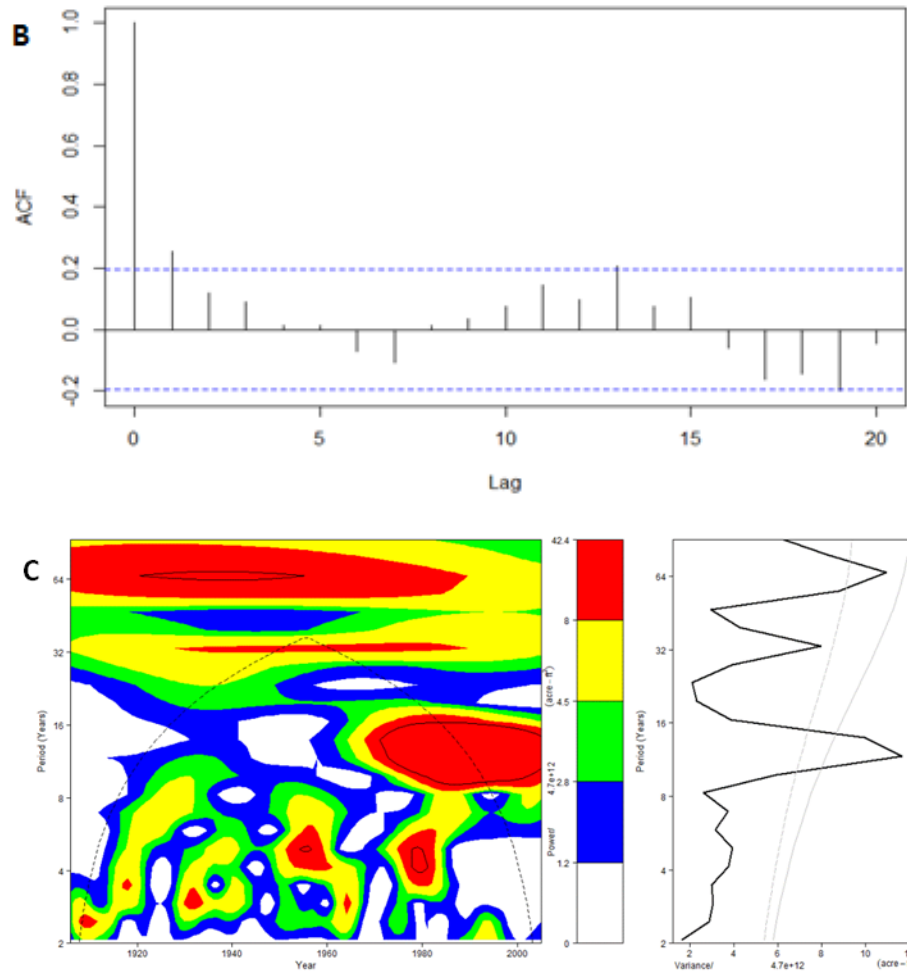
Figure 1. (A)The time series of the historical streamflow at Lees Ferry, AZ (1906-2005). (B) Autocorrelation function of the historical streamflow at Lees Ferry. (C) Wavelet and global spectrum of the historical streamflow at Lees Ferry.

The wavelet spectrum (left) reveals the time varying spectrum and the strength of the various periodicities while the global spectrum (right) highlights the average strength of each signal over the entire timeframe. In the Lees Ferry data, the global spectrum shows significant peaks in the 8-16 year band, as well as in the 64-year band. The gray lines in the global spectrum indicate a 90% and 95% confidence interval while the dashed line in the local spectrum outlines the cone of influence. The confidence intervals are based on a AR(1) model which is a

8

conservative null model and widely used in climate studies, as opposed to white noise which is prescribed in statistical literature. Regions beyond the cone of influence should be interpreted with caution, as they are likely influenced by boundary effects resulting from padding the data with zeros to create a cyclic time series necessary for applying the Fourier transform during wavelet analysis [*Torrence and Compo*, 1998]. It is of interest that the auto correlation function (Figure 1B) of the streamflow (Figure 1A) exhibits a weak lag-1 autocorrelation, yet it has significant low frequency variability.

Once the statistically significant frequencies of each band are identified, the time series is filtered at each frequency and are combined to create a 'band passed' time series which is obtained as follows:

$$x_t = \frac{\delta_j \delta_t^{1/2}}{C_\delta \Psi_0(0)} \sum_{j=0}^{J} \frac{\Re\{X_t(a_j)\}}{a_j^{1/2}} \quad \textbf{Equation 3}$$

where the real parts of the wavelet transform are summed over all scales (i.e., period), $j = 1:J$, and multiplied by a coefficient consisting of the scale averaging coefficient, δ_j, the sampling period, δ_t, and two empirically derived factors, C_δ and $\Psi_0(0)$, specifically related to the Morlet wavelet [*Torrence and Compo*, 1998]. By limiting the scale of the summation, j, specific "band" reconstructions can be computed. Thus obtained band passed series are summed and its difference from the original series provides the 'residual' series. The band passes and the residual series together recover the original flow series.

For the Lees Ferry flow, based on the wavelet spectrum (Figure 1C) there are two significant bands as mentioned above – 8-16 year and 64-80 year. Using all the frequencies in the respective

bands, apply Equation 3 the resulting band passed series and the residual series are shown in Figure 2.
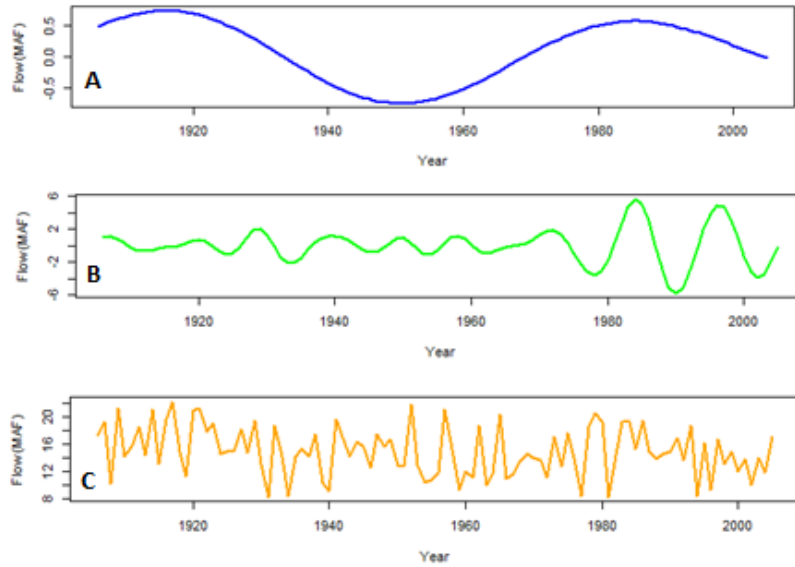
Figure 2. Band passed time series for the historical Lees Ferry, AZ streamflow. (A) Decomposed band for 64-80 year period. (B) Decomposed band for 8-16 year period. (C) Noise band.

In the WARM framework, these bands are modeled and simulated using traditional autoregressive models [*Kwon et al.*, 2007]. Results from the WARM framework include an ensemble of streamflows each of which reflects the stationary characteristics of the decomposed components.

2.2 Enhancements to the WARM Framework

While the WARM simulations adequately capture key global spectral properties, they fail to capture non-stationary features [*Nowak et al.*, 2011], such as the power in the 8-16 year band restricted to recent decades. To improve upon this, *Nowak et al.* developed an enhanced WARM framework that incorporates the Scale Average Wavelet Power (SAWP). The SAWP is the

average variance of a decomposed band that can be computed at each time step and is given by the following equation:

$$\bar{X}_t^2 = \frac{\delta_j \delta_t}{C_\delta} \sum_{j=j_1}^{j_2} \frac{|X_t(a_j)|^2}{a_j} \qquad \textbf{Equation 4}$$

where j_i and j_2 are the scales over which the average is computed [*Torrence and Compo*, 1998]. Essentially, the SAWP captures the strength of the temporal variability present in the time series data. The square root of this is equivalent to the standard deviation at a given time step for the band. For illustration purposes, the SAWP corresponding to the 8-16 year period band identified in the Lees Ferry historical streamflow data is shown in Figure 3.
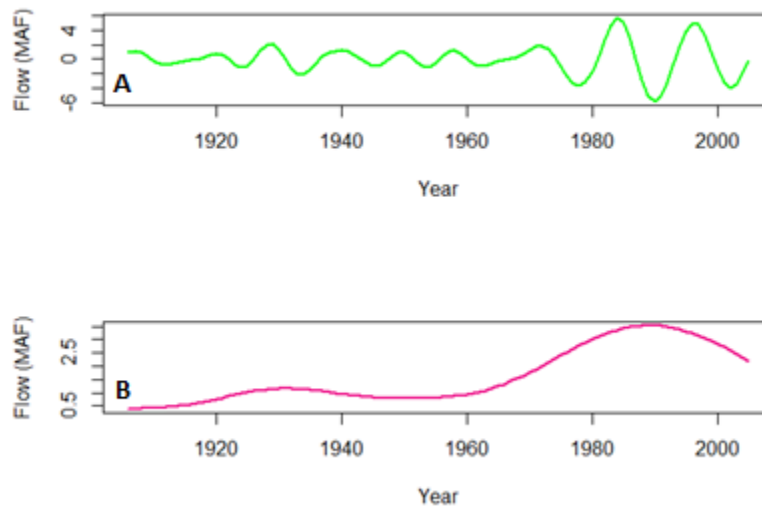
Figure 3. The decomposed band series for the 8-16 year period for the historical streamflow at Lees Ferry, AZ (same as Figure 2B) and (B) the corresponding SAWP.

Notice that the band series exhibits higher variability in recent decades (top figure) and the SAWP (bottom figure) reflects this very well.

In the enhanced WARM framework, the band series are divided by the square root of their respective SAWP to transform them into stationary components. Thus obtained stationary components can be well modeled using lower order AR models as in the WARM approach. Upon simulation, the components are multiplied by the square root of the SAWP to transform them back into non-stationary time series, thus capturing the temporal variability present in the original decomposed bands. This process is outlined in Figure 4.
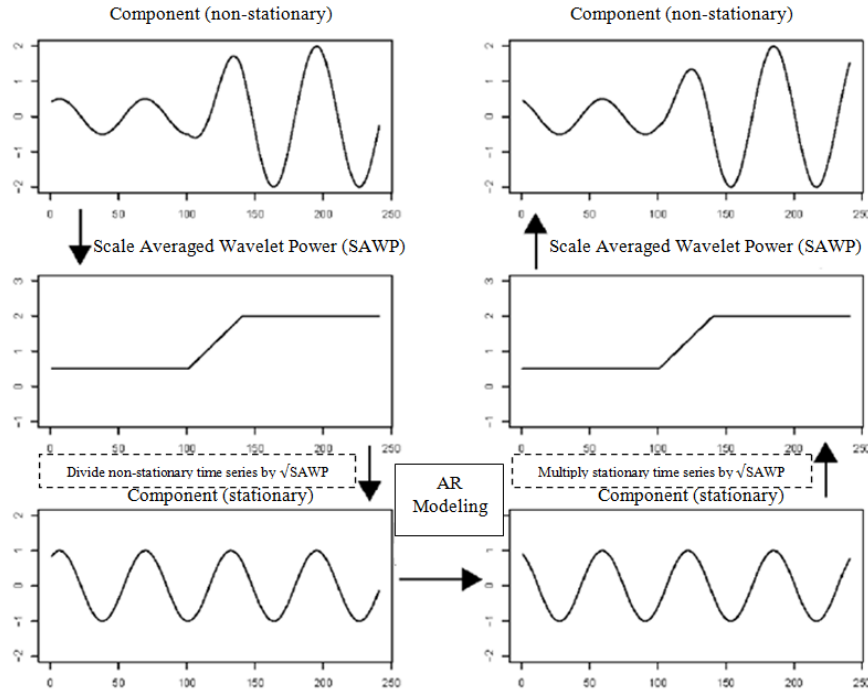
Figure 4. Outline of the enhanced WARM framework developed by *Nowak et al.*, 2011.

This reconstruction process is applied to all of the decomposed time series components, except for the noise. Similar to the WARM framework, the enhanced WARM framework is complete once the noise and the reconstructed bands are summed together, resulting in a simulated time series that incorporates temporal variability. Preserving this temporal variability is important, as recent research suggests linkage between decadal signals present in Lees Ferry

streamflow data and large scale climate indicators [*Nowak et al.*, 2012]. For details on the enhanced WARM framework refer to *Nowak* et al., 2011.

2.3 Improvements to the Enhanced WARM Framework

While both the enhanced and original WARM frameworks provide a method for identifying variability and simulating based on traditional linear time series models, nonlinearities are present in time series data. The use of autoregressive models for simulation limits our ability to simulate non-stationary data based on specific timestep characteristics. Furthermore, the enhanced WARM framework provides a method for simulating the features of the historical series, but fails to simulate future periods in which the SAWP remains unknown. The goal of this research is to develop a projection methodology that identifies time step-specific wavelet characteristic associated with variability cycles, and based on those characteristics, create more skillful projections that can be used to inform the decision-making process. Given the limitations of both the enhanced and original WARM frameworks coupled with the objectives of this research, we developed a new technique that characterizes variability at any timestep, and based on that characterization, projects future variability.

Our methodology modifies the enhanced WARM framework which consists of three broad steps (i) wavelet decomposition of the time series to band series, as described in previous section, (ii) time varying SAWP and phase angle for each band series and (iii) K-nearest neighbor time series resampling for mutlidecadal simulation.

2.3.1 Wavelet Analysis

In this section we summarize our application of wavelet analysis—which stems from both the original and enhanced WARM frameworks previously discussed [*Nowak et al.,* 2011;

Kwon et al., 2007]. Using Equations 1 and 2, a time series can be decomposed to identify the statistically significant spectral peaks. Although this work incorporates the Morlet wavelet (Equation 2), different wavelets can be selected based on individual application and preference [*Torrence and Compo*, 1998]. Once identified, Equation 3 is applied to create filtered 'band passed' time series, which can be summed and subtracted from the original time series to create a 'noise' band.

2.3.2 SAWP and Phase Angle Computations

To create skillful projections of each band, properties of the bands that correlate to specific time steps, $t = 1, ..., N$ must be identified. This methodology uses the SAWP (Equation 4) and phase angle to accomplish this. As previously discussed, the SAWP is defined as the average variance of the signal versus time—thus inherently incorporating frequency modulation within a time series [*Torrence and Compo*, 1998]. For time t, the SAWP is calculated for each of the significant spectral peaks identified during the wavelet analysis.

Similarly, the phase angle of each band for time step t. Because the wavelet transform (Equation 1) is complex, we can define it in terms of the real, $\Re\{X_t(a_j)\}$, and imaginary, $\Im\{X_t(a_j)\}$ parts [*Torrence and Compo*, 1998]. Given these terms, the phase angle equals:

$$\tan^{-1}\left(\frac{\Im\{X_t(a_j)\}}{\Re\{X_t(a_j)\}}\right) \quad \textbf{Equation 5}$$

Because the bands span many scales (e.g., 8 to 16 year period), a weighted average of the phase angle is computed as the representative phase angle for the band at each time step – the SAWP values of each period within the band are used as weights. For example, for the 8-16 year

period, the phase angle is calculated for each scale—8, 9.5, 11.3, 13.5, and 16—and a weighted average is computed for the respective period and later used during for a K-Nearest-Neighbor (KNN) resampling algorithm described below.

2.3.3 K-Nearest-Neighbor (KNN) Resampling Algorithm

Using the SAWP and phase angle calculations, we implement a KNN algorithm to project each of the bands for multiple decades. In general, the KNN algorithm uses a user-defined feature vector, $\boldsymbol{D}_t$, at time step t, to find the historical nearest neighbors of this current feature vector. The k nearest neighbors are determined by calculating the Euclidean distance between the feature vectors of the past, $\boldsymbol{D}_i$, and the current feature matrix, $\boldsymbol{D}_m$. The Euclidean distance is given by:

$$r_{im} = \sqrt{\left[\sum_{j=1}^{d}\left(v_{ij} - v_{mj}\right)^2\right]} \quad \textbf{Equation 6}$$

where $v_{()j}$ is the jth component $\boldsymbol{D}_{[]}$ [*Rajagopalan and Lall*, 1999, *Lall and Sharma,* 1996].

Once identified, the set of nearest neighbors $j_{i,k}$ are ordered and weighted such that the nearest neighbor to the current feature vector has the highest weight and the farthest neighbor the lowest weight. A commonly-used weighting metric was developed by *Lall and Sharma* (1996) and given as:

$$K[j[i]] = \frac{1/j}{\sum_{j=1}^{k} 1/j} \quad \textbf{Equation 7}$$

where $K[j[i]]$ is the probability assigned to the specific neighbor, $j[i]$.

Using the probability function above, one of the historical neighbors is selected – consequently, its time step, say, *Ts*. The entire series segment starting at *Ts* up to a desired length, say *Ts+T,* is resampled as the simulated series. This process is repeated to generate ensembles. Here, we apply this resampling to each of the band passed series separately. The residual series is resampled at random since it has no structure. Thus, simulated series are summed to obtain simulations of the original series.

The feature vector chosen is the SAWP and phase angle (PA) values. For illustration purposes, let time series x_t be comprised of three different bands: two significant peaks from the spectral analysis ($y_{1,t}$ and $y_{2,t}$) and one corresponding noise band ($y_{n,t}$). The feature vector (**f**) for band $y_{1,t}$ is as follows:

$$\mathbf{f} = \left[SAWP_{y1,t}, PA_{y1,t} \right] \quad \textbf{Equation 8}$$

The corresponding feature matrix (**F**) is comprised of the band's remaining SAWP and phase angle values—excluding those contained in the feature vector (**f**). For $y_{1,t}$ the feature matrix would look like:

$$\begin{bmatrix} SAWP_{y1,t=0} & PA_{y1,t=0} \\ \vdots & \vdots \\ SAWP_{y1,t=n} & PA_{y1,t=n} \end{bmatrix} \quad \textbf{Equation 9}$$

Using the feature vector and matrix, the *K* nearest neighbors are determined and weighted according to the method previously described. The KNN is then used to resample the

corresponding decomposed band passed time series. The noise is simulated per the methodology described in the WARM approaches [*Nowak et al.*, 2011; *Kwon et al.*, 2007].

2.4 Application and Data Set

The utility of this projection methodology is demonstrated using the paleo reconstructed streamflow data at Lees Ferry, AZ (1490-1905) combined with historical natural flow data spanning from 1906-2010 [*Woodhouse et al.*, 2006; *U.S. Bureau of Reclamation*, 2013]. The paleo reconstructed data provides a robust view of the past as it spans more than 500 years of data and is derived from fitting linear regression models to tree-ring chronologies in the Colorado River Basin. Additionally, the observed natural flow data, ranging from 1998-2010, is computed by removing anthropogenic impacts—such as reservoir regulation and consumptive water use—from the recorded historical flows updated and maintained by the U. S. Bureau of Reclamation. For an in-depth discussion on the reconstruction or the naturalized flow methodologies, readers are referred to *Woodhouse et al.* (2006) and *U.S. Bureau of Reclamation* (2013).

This data set was selected because previous research links large scale climate forcings to the hydrologic variability present in the Upper Colorado River Basin. Using annual Lees Ferry streamflow data and wavelet spectral analysis, *Nowak et al.* (2012) identified two dominant spectral peaks—a low frequency component occurring around the 64 year period coupled with a higher frequency, non-stationary, decadal signal occurring around the 8 to 16 year period (Figure 1). Further analysis links the decadal signal with precipitation variability coinciding with large scale climate forcings occurring in the Pacific Ocean—specifically, the Pacific Decadal Oscillation. Similarly, the lower frequency signal shows a weaker correlation to temperature variability and the Atlantic Multidecadal Oscillation (AMO). Given the importance of these low

frequency periods, we propose that good projections of these periods can enable realistic multidecadal projections of streamflow.

2.5 Discussion and Results

Using the Lees Ferry streamflow record (1490-2010), wavelet spectral analysis reveals three significant frequency bands—a low frequency component occurring at the 60-118 year period, a moderate frequency component occurring at the 20-52 year period, and a higher frequency decadal signal occurring at the 7-14 year period (Figure 5).
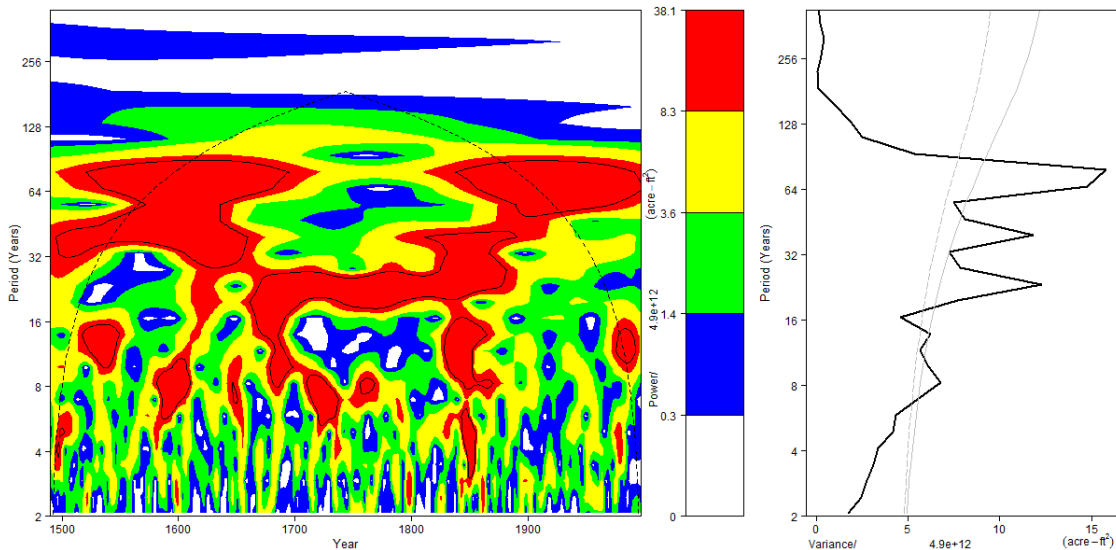
Figure 5. Wavelet and global spectrum of the streamflow at Lees Ferry, Arizona using the paleo reconstructed streamflow (1490-1905) combined with the historical natural flow (1906-2010).

Using the equations described earlier, the band passed components and the corresponding SAWP are obtained and shown in Figure 6.
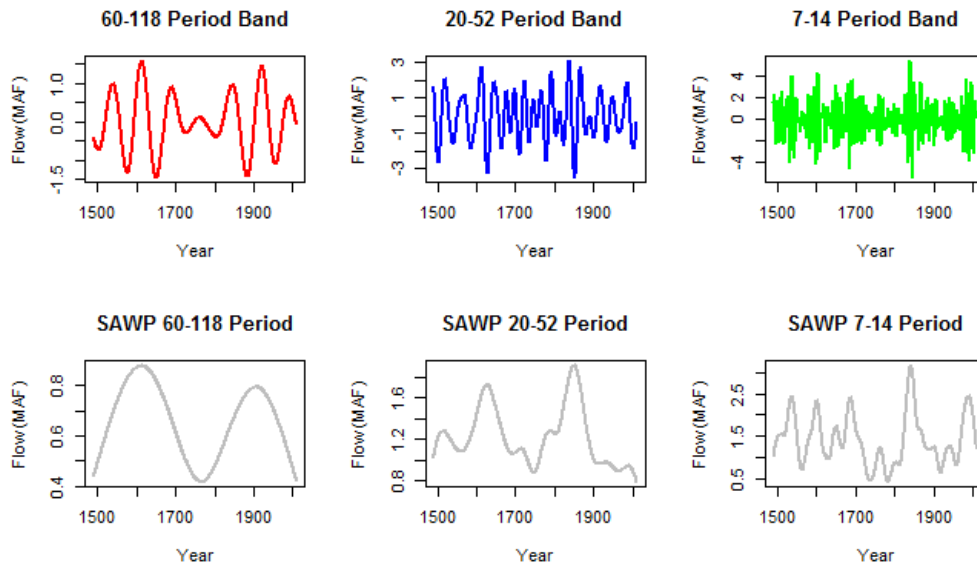
Figure 6. Decomposed bands and corresponding SAWPs for the streamflow at Lees Ferry, AZ (1490-2010).

Notice that the SAWP effectively reflects the variability present in the decomposed time series.

To validate the proposed methodology, the wavelet analysis was performed on data prior to 1906 and using the KNN resampling algorithm with the feature vector of 1905, 500 simulations were made for the 100-year period (1906-2005) for each band separately and the residuals – together providing 500 ensembles of the bands and the streamflow. Figure 7 shows boxplots of the decadal band simulations overlaid with the observed band passed time series corresponding to the projection period (1906-2005). The 'observed band' for this period is obtained by performing the wavelet analysis for this period separately. Note, the projection methodology can be applied to any time scale greater than five years; however Figure 7 illustrates 100 year projections.
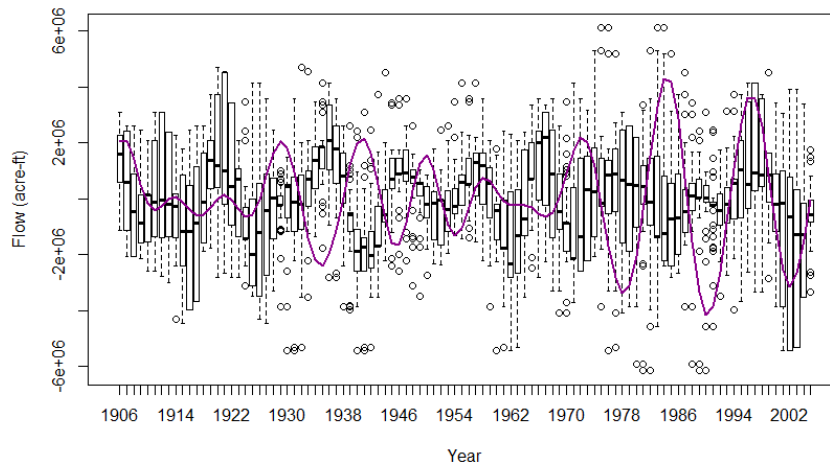
Figure 7. Boxplot of the simulated projected band for the 8-16 year period for Lees Ferry, AZ overlaid with the observed band (1906-2005).

As illustrated in Figure 7, the simulations effectively capture the observed variability of the decadal band. However, the amplitude modulation and the phase are not captured throughout the period. Figure 8 illustrates the simulated flows as boxplots along with observed flow. The simulated flows capture the overall variability of the observed and they also reproduce the long term decreasing trend present in the observed. As with the decadal band simulations, amplitude modulation over time and the phase are not well reproduced. The 100-year simulations are based on spectral characteristics at a given year (in this case, 1905) – the phase and amplitude modulation of the 100-year simulations will only be captured if the underlying dynamics of evolution of the streamflow is close to being periodic. Given this is not the case we do not expect the amplitude and phase modulations to be captured in the simulations. However, we could expect to capture broadly the statistics and global spectral features.
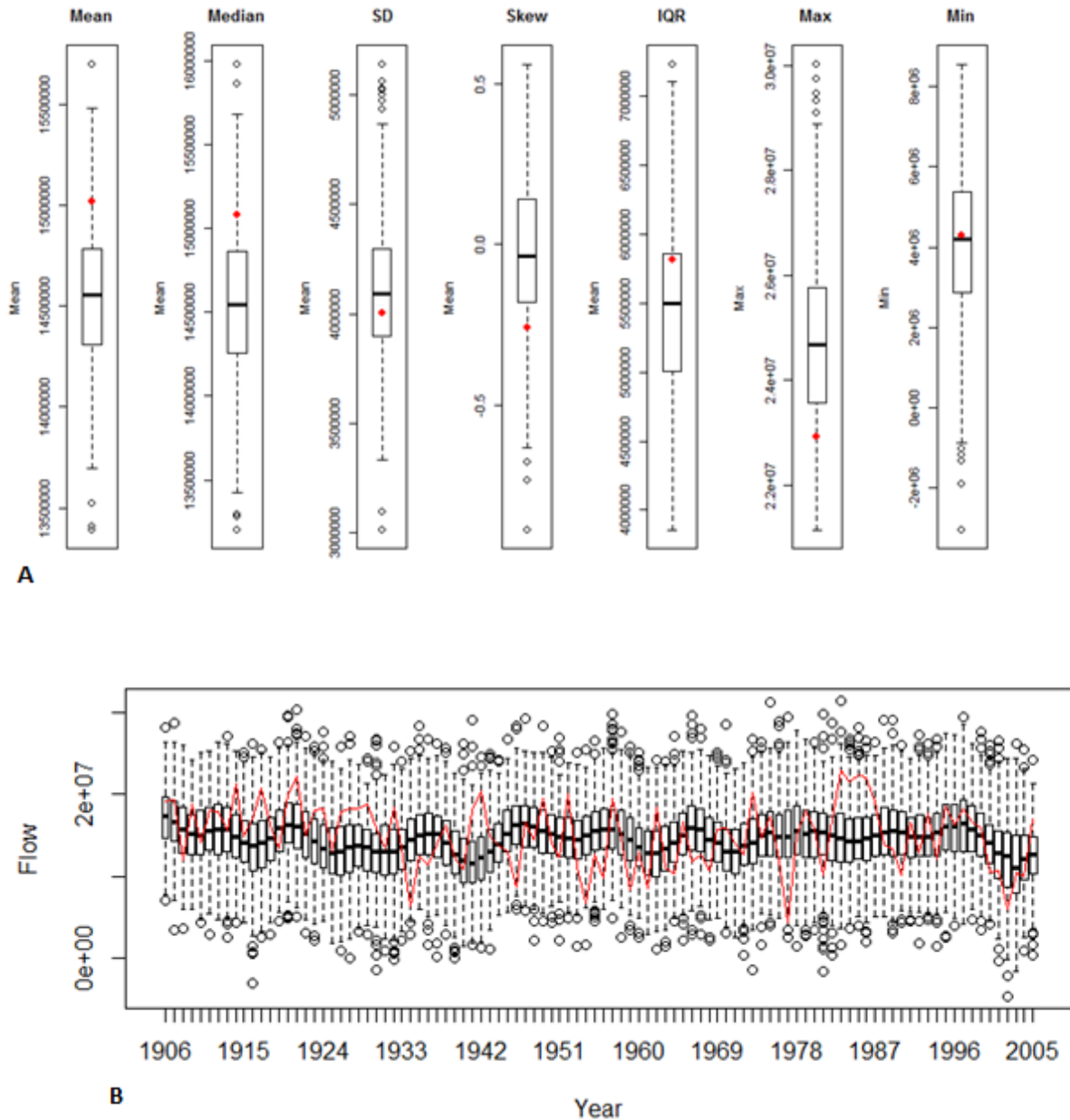
Figure 8. (A) Boxplots of the standard statistics of the simulated projected streamflows at Ferry, AZ overlaid with the observed (1906-2005) and (B) Boxplots of the simulated projections overlaid with the observed.

A suite of basic distributional statistics from the simulations are computed and shown as boxplots along with the corresponding stats of the observed flow. The mean and median are under simulated while the standard deviation is well captured and so is the interquartile range.

21

The skew and minimum values of the observed are just outside the interquartile range of the simulations. The distributional properties are fairly well reproduced by the simulations.

To evaluate the spectral features of the simulations, global wavelet spectra of the simulations are computed and shown with that of the observed in Figure 9. The simulations have power at the decadal and higher periodicities as in the observed. The three dominant periodicities in the simulations are those present in the paleo record (Figure 5) used in the simulation. The spectral peak at the decadal band is well reproduced (the red and blue lines), however the lower frequency bands (i.e. higher periods) are simulated strongly compared to the observations. This tends to be the case, because the simulations have the low frequencies in all the simulations—thus giving them more spectral power, whereas in the observations the low frequencies are weakly present. We focus more on the reproduction of the decadal band features than the lower frequencies.
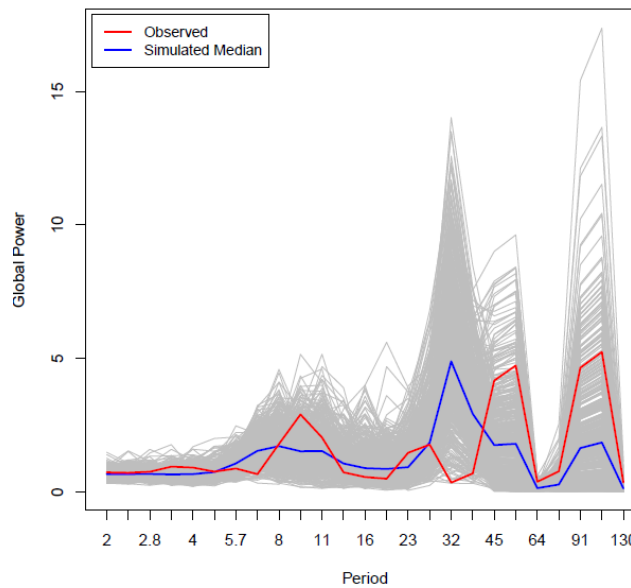
Figure 9. Plot of the global spectrum of the projected simulated streamflow for Lees Ferry, AZ overlaid with observed (red) and the simulated median (blue).

22

Furthermore, a spectral plot of the median of the simulated flows (Figure 10A) compared to the spectrum of the observed historical flow (Figure 1C) for Lees Ferry highlights that the lower frequency components, especially the peak in the decadal band is well preserved in the projection methodology. However, the non-stationarity of this band present in the observations is not reproduced in the simulations. Given that the simulations are made for a 100-year period such spectral non-stationarities are not expected to be captured. Considering that these simulations are blind for the 100-year period, the ability to reproduce broad spectral features—such as the decadal band—is noteworthy as these bands can be used to inform the decision-making process for water resource managers.

In a typical time series simulation, such as with WARM or enhanced WARM where the features of the observed data are incorporated in the model which are then used to simulate, these features are all well produced (e.g., *Nowak et al.,* 2011).

A

B
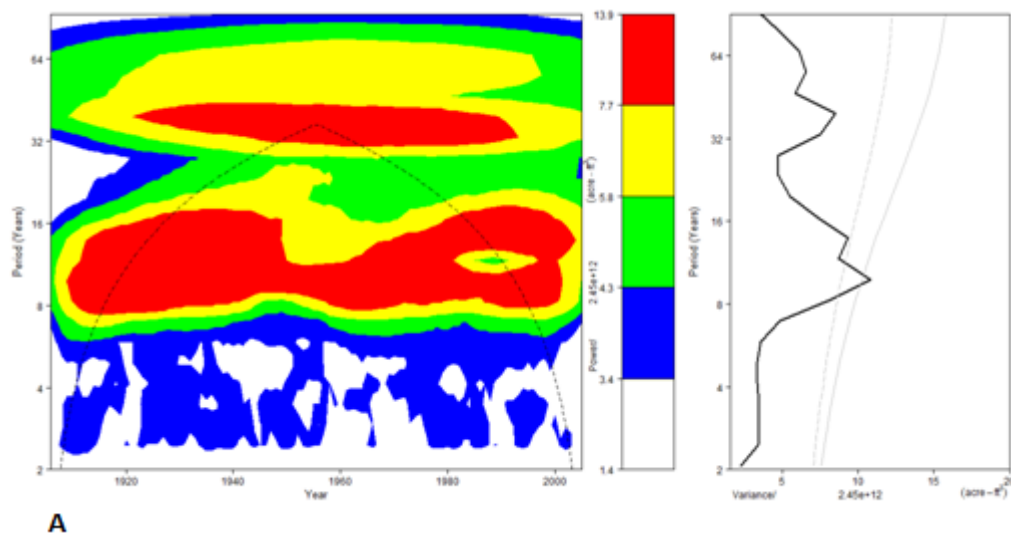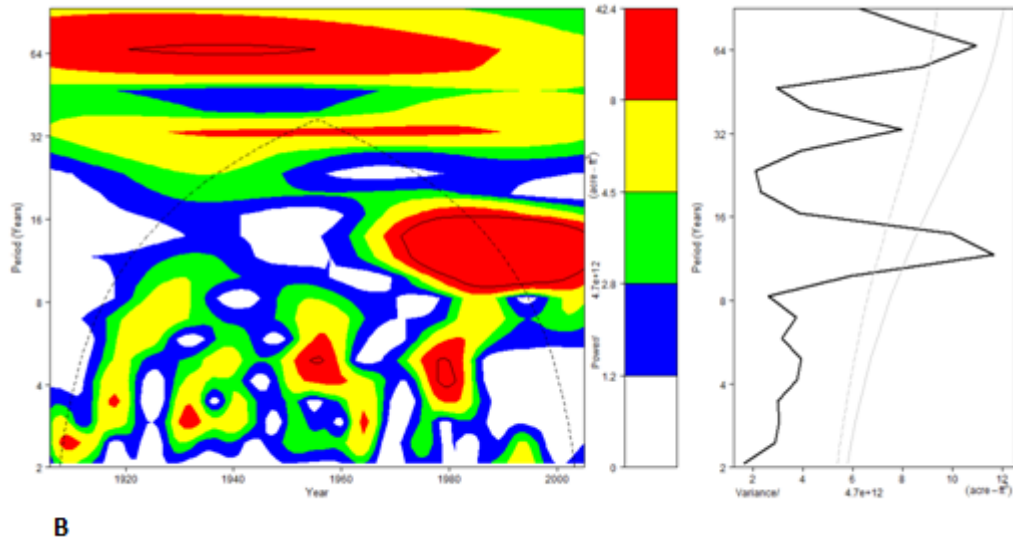
Figure 10. (A) Wavelet and global spectrum of the median simulated streamflow at Lees Ferry, AZ compared to (B) the wavelet and global spectrum of the observed streamflow at Lees Ferry, AZ (1906-2005).

In addition to the historic record, analysis of three hydrologic epochs—1585 to 1634, 1780 to 1829 and 1940 to 1989—are made, as they respectively represent high, average and low flow epochs. Figures 11-13 illustrate wavelet spectrum, the simulated band projections compared to the observed bands, as well as the simulated flow projections compared to the observed flow for three different hydrologic epochs. These projections are essentially blind projections in that the period of interest (i.e., the projected period) is removed from the paleo record and simulated based on the remaining data.
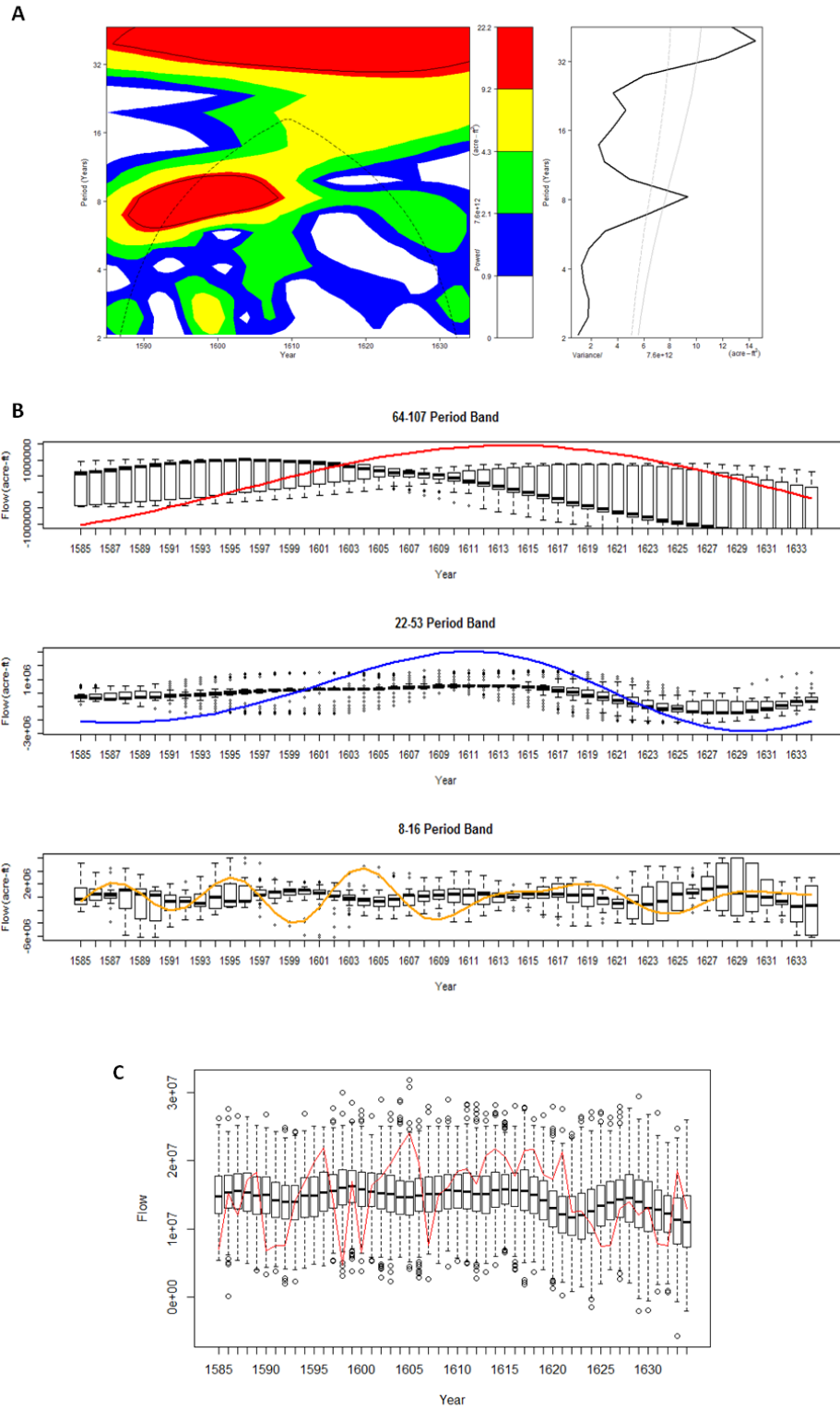
Figure 11. (A) Spectrum of the 1585-1634 paleo streamflow data. (B) Boxplot of the projected decomposed bands for Lees Ferry, AZ during a high flow epoch compared to the observed (1584-1634). (C)Boxplot of the simulated flows compared to the observed (1584-1634).
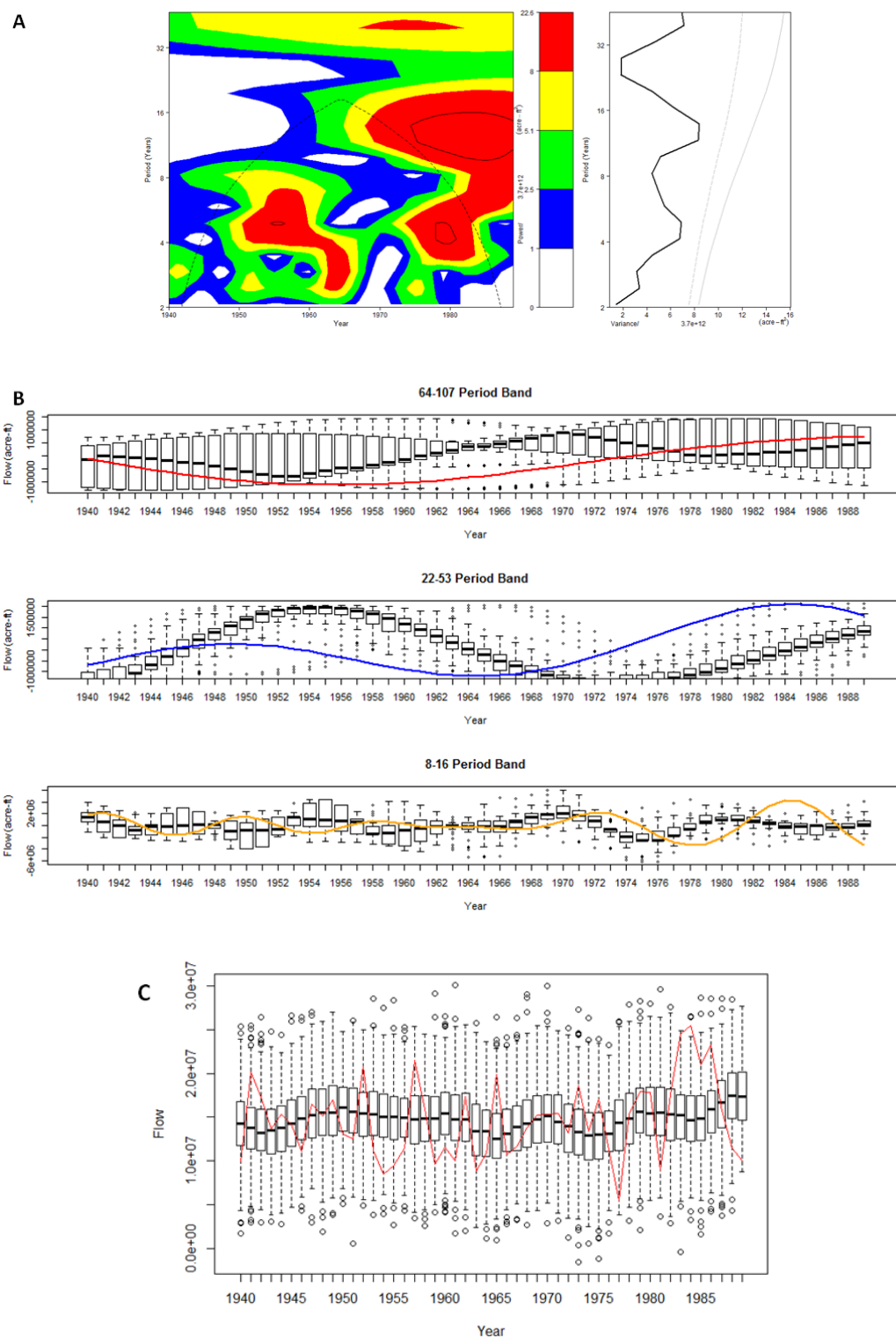
Figure 12. (A) Spectrum of the 1939-1989 historic streamflow data. (B) Boxplot of the projected decomposed bands for Lees Ferry, AZ during an average flow epoch compared to the observed (1939-1989). (C) Boxplot of the simulated flows compared to the observed (1939-1989).
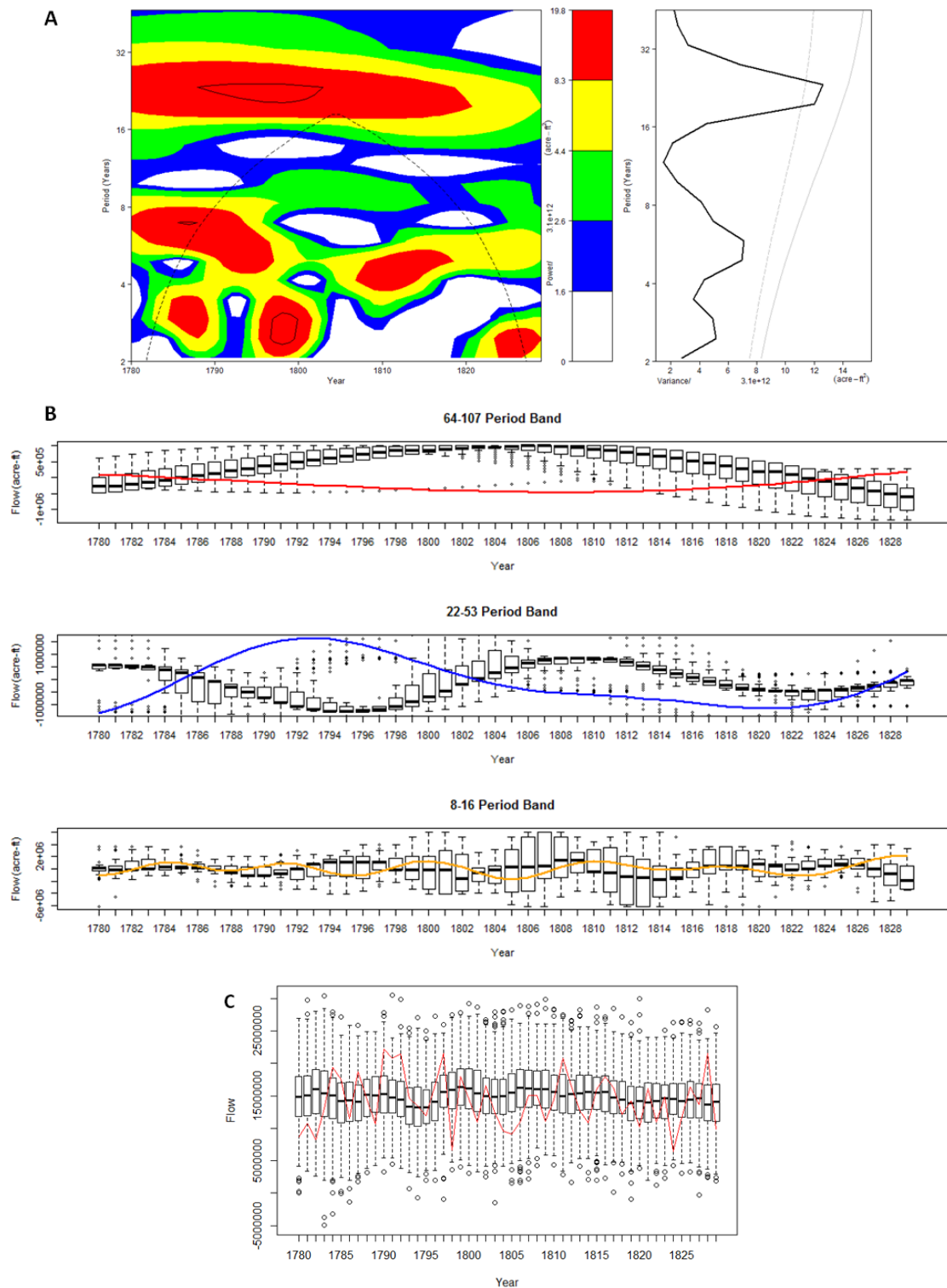
Figure 13. A) Spectrum of the 1779-1829 paleo streamflow data. (B) Boxplot of the projected decomposed bands for Lees Ferry, AZ during a low flow epoch compared to the observed (1779-1829). (C) Boxplot of the simulated flows compared to the observed (1779-1829).

As evident in Figures 11-13, and similar to simulations for the modern period, the simulations capture the variability of the bands but do not capture the amplitude modulation and phase. Differences exist in both the amplitude and phase of the projected bands compared to the observed bands. This is a typical problem due to boundary issues in any filtering method including wavelets [*Rajagopalan et al.,* 1997]. Filtering is done within a window, in this case, within the window of the wavelet, thus at the end of the time series the filtering is performed with fewer observations – hence, the boundary bias. There are adhoc solutions to the boundary problem but none satisfying – thus, the inability to capture the amplitude and phase modulations. Therefore, evaluating the simulations for their global spectral properties and over a longer period of simulation obviates this issue, but for shorter simulation period this is stark. This is seen in our simulation results above, where the distributional and spectral properties are better captured over a longer period of simulation – thus, enabling their utility in long term planning.

To assess how these projections differ from climatology, a rank probability skill score (RPSS) was computed. The RPSS is a commonly used verification metric that measure performance of ensemble predictions in probabilistic terms and is based on the rank probability score (RPS). To estimate the RPS, the prediction variable (i.e., streamflow) is classified into k mutually exclusive and exhaustive categories. The forecast and observed probabilities corresponding to those categories are then estimated using the following equation:

$$RPS = \sum_{i=1}^{k}\left[\left(\sum_{j=1}^{i} p_j - \sum_{j=1}^{i} d_j\right)^2\right] \quad \textbf{Equation 10}$$

where the forecast probabilities, p_j, are the proportion of ensembles falling into each category, and the observed probabilities, d_j, equal one if the observation fall into the kth category and otherwise zero.

Given the RPS, the RPSS indicates how the predictions perform relative to climatology and is given as:

$$RPSS = 1 - \frac{RPS\ (prediction)}{RPS\ (climatology)} \qquad \textbf{Equation 11}$$

The RPSS ranges from negative infinity to positive one. Positive RPSS scores indicate the prediction accuracy performs better than climatology; zero indicates the same as climatology; and negative values indicate the prediction accuracy performs worse than climatology. For this work, 50 year projections were created from 1512 to 1960. Because the projection methodology is designed to capture the overall trends—not the annual to inter-annual trends—the mean of each 50-year projection period was computed and compared to the mean of the corresponding period in the paleo record. The overall RPSS of the 50-year projections equals 0.18. To capture the RPSS values at a more finite resolution, the projections periods were broken into different sets—each set containing 15 projection periods (e.g. set one contains the 1512-1526 projections). A boxplot of these RPSS values is shown below (Figure 14).
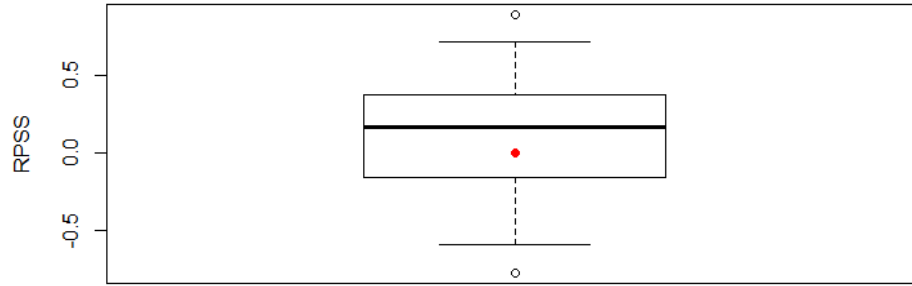
Figure 14**. Boxplot of the RPSS for the simulated streamflow projections (1512-1960). Red dot represents climatology.**

The median RPSS value equals 0,27—indicating the projections are skilful at simulating the categorical mean flow. Again, this methodology aims at capturing the overall trends of a projection period—not the annual to inter-annual trends. The RPSS values indicate these projection accomplish this and perform slightly better than climatology.

2.6 Climate Change Application

Thus far, the proposed methodology uses the paleo reconstructed record to project the decomposed bands—making an assumption that future trends and variability mimic historic patterns. However, climate research suggests these trends and variability may deviate from history. Currently, there is a need for novel projection methods that incorporate both natural variability and climate change trends, as projections from general circulation models [GCMs] inadequately predict inter-decadal climate signals—which are often drivers of hydroclimatic variability [Nowak *et al.,* 2012; *Timilsena et al.*, 2009; *McCabe et al.*, 2007; *Hidalgo and Dracup*, 2003; *Cayan et al.*, 1999; *McCabe and Dettinger*, 1999; *Piechota et al.*, 1997]. This method can be adapted to address this gap.

Once streamflow projections are developed using the aforementioned methodology, climate change trends can easily be applied. To do this, we remove important climatological

components from the projections by subtracting the series mean and dividing by the standard deviation—resulting is scaled "anomalies" [Rajagopalan *et al.,* 1997]. We then compute the mean and standard deviation from 112 downscaled GCM projections for Lees Ferry [*IPCC Fourth Assessment Report, 2007*]. The climate-trended mean and standard deviation are then applied to the scaled anomalies, resulting in streamflow projections that contain the inter-annual to inter-decadal climate signals as well as climate change trends. Note, any climate trends can be applied using this method.

2.7 Conclusion and Future Work

Generating decadal scale projections is a nascent field, fraught with complex challenges. Some of these challenges are evident in this methodology—as it proves difficult to project the phase angle and amplitude of each quasi-periodic band. Although the proposed methodology attempts to address some of these challenges by integrating phase angle information into the prediction process, it does not prove effective enough, as the proposed methodology only performs slightly better than climatology.

Furthermore, while the proposed methodology takes into consideration where we currently stand in the quasi-periodic cycle and creates predictions based on that knowledge, the irregularity of the cycles presents a grand challenge to the climate community. Tackling the challenge from a different angle, future work could focus on understanding the physical processes that drive decadal variability and integrating that information into projection methodologies. This could include better understanding how decadal variability in ocean processes impacts large scale climate indicators. Or, better understanding how anthropogenic forcings interact with natural variability—with a focus on decadal time scales [*Solomon et al.*, 2011].

Despite the skill of the proposed methodology, information derived from decadal scale projections can be used to inform decision-making logic. Chapter 3 presents a framework that integrates this information and demonstrates its utility for aiding in flexible, iterative, adaptive management.

CHAPTER 3: APPLICATION OF DECADAL SCALE PROJECTIONS TO MANAGEMENT IN THE GUNNISON AND UPPER COLORADO RIVER BASINS

This chapter describes the development of a robust decision-making framework that incorporates the decadal projections presented in Chapter 2. This decision-making framework is applied to the Upper Colorado River (headwater to the Colorado-Utah state line) and the adjacent Gunnison River Basin, a tributary to the Upper Colorado. By applying the framework to two different river basins, we hope to demonstrate the utility of incorporating decadal scale information in the decision-making process, as well as the role of storage in decadal scale planning. The results of this case study are presented in Chapter 4.

3.1 Introduction

In light of climate change and the associated uncertainties, flexible and adaptive resource management strategies are becoming increasingly important by allowing water managers to more easily assess and respond to the associated outcomes. While the objectives of flexible management vary regionally, in the southwestern United States water supply reliability and mitigating shortages are of upmost importance and the primary objective of current adaption strategies [*Gober and Kirkwood,* 2010; *Ragajopalan et al.,* 2009; *Miller et al.,* 1994].

The importance of system reliability is highlighted in the Bureau of Reclamations' Colorado River Basin Water Supply and Demand Study (Basin Study), which describes the challenges and opportunities for managing and mitigating shortages in the Colorado River system given the likelihood of increasing demands coupled with reduced supply projections. Throughout the Basin Study, signposts were developed to detect system vulnerabilities before they occurred. The triggering of a signpost signified the need for implementing various

management strategies [*Bureau of Reclamation*, 2012]. The proposed decision-making framework incorporates a different approach to dealing with system vulnerability. Instead of using signposts to detect impending vulnerabilities, the decision-making framework links system vulnerability to projected ten-year streamflow conditions. Therefore, if water managers understand the relationship between hydrologic conditions and system performance, they can use this knowledge to drive the decision-making process.

With a focus on the Upper Colorado River and the Gunnison River Basin, this work demonstrates the utility of incorporating decadal scale streamflow projections into a robust decision-making framework designed to increase system reliability and reduce basin shortages by making the information from these projections available to the decision making logic. The proposed framework is based on the fundamental idea that if decision-makers have access to more skillful projections—incorporating both natural variability and GCM-informed climate change trends— they can use this information to drive the decision-making process, allowing for more adaptive and flexible management.

3.2 Gunnison River Basin

The Gunnison River basin (GRB) is located in southwest Colorado (Figure 16) and drains approximately one-quarter of Colorado's Western slope (7,960 mi^2). With basin elevations ranging from 4,550-14,300 ft, the Gunnison River originates along the Continental Divide and flows west towards Grand Junction, Colorado, where it joins the Colorado River. On average, the GRB's total annual volume of runoff is approximately 1.8 million acre-feet—making it the fifth largest tributary of the Colorado River. Like much of the West, the Gunnison River no longer flows unimpeded, as it is dammed by the Aspinall Unit which consists of three dams and the

associated Blue Mesa, Morrow Point and Crystal reservoirs, and Taylor Park Dam further upstream.

The Aspinall Unit spans 40 miles of the Gunnison River and comprises the basin's primary water resources development. The project provides water for hydroelectric power, flat-water recreation, agricultural irrigation, instream use (i.e. fish and wildlife), municipal water supply, and meeting Colorado River compact requirements [*Gunnison Basin Water*, 2003].

The Aspinall Unit's three reservoirs have a combined storage of approximately 1.1 million acre-feet and hydropower generation capacity of 287 megawatts.
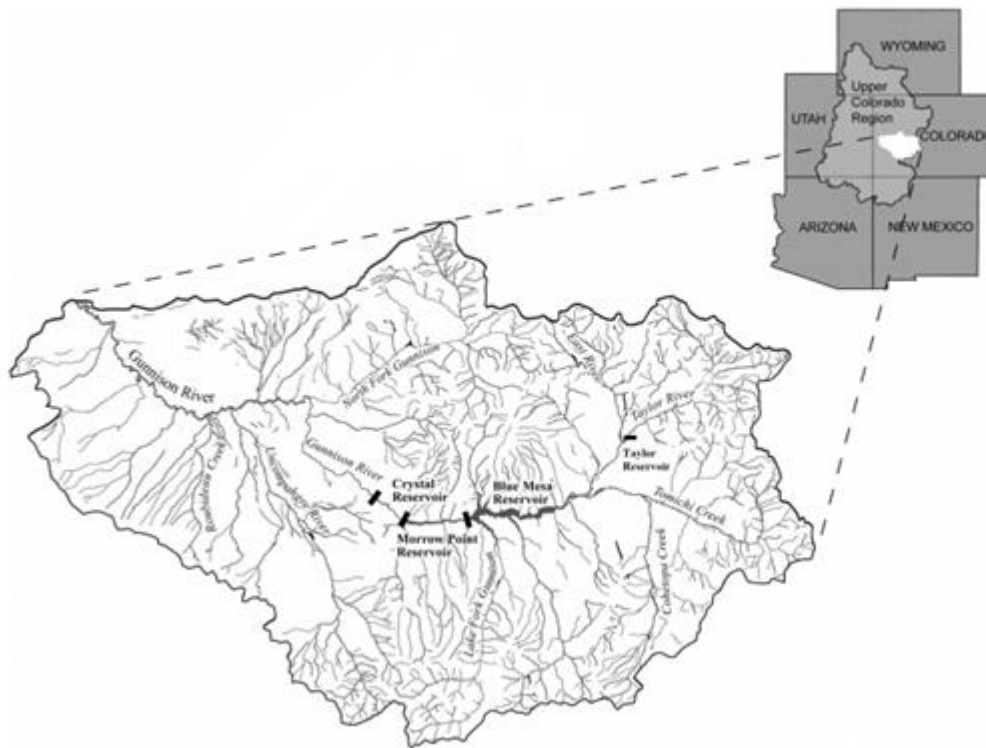
Figure 15. Map of the Gunnison Basin Hydrologic Unit with the black rectangles representing the four reservoirs.

The Bureau of Reclamation operates the Aspinall Unit to satisfy multiple objectives and competing demands. Typically, reservoir storage levels are drawn down during the fall and winter months, and re-filled with spring snowpack run-off. Throughout summer, Reclamation attempts to maintain steady reservoir levels to maximize flat water recreation on Blue Mesa Reservoir, while simultaneously releasing enough water to meet downstream demands. Further, hydropower generation is maximized throughout the year [*Gunnison Basin Water,* 2003].

In addition to the Aspinall Unit, Taylor Park reservoir is located upstream of the Blue Mesa reservoir on the Taylor River. Taylor Park serves primarily as a storage reservoir, with a storage capacity of 106,200 acre-ft. Taylor Park is part of the Uncompahgre Project, which stores water in the Taylor Park and diverts it through the Gunnison Tunnel (located downstream of Crystal Reservoir) for delivery to farmers and ranchers in the Uncompahgre Valley. On average, the project diverts 325,000 to 365,000 acre-feet of water per year.

3.3 Upper Colorado River Basin

The Colorado River originates near the Continental Divide (14,000 ft) in Colorado and flows southwest towards the Colorado-Utah state line (4,300 ft), eventually reaching the Sea of Cortez in Mexico. Often considered the lifeline of the American Southwest, the Colorado River supplies water for nearly 40 million people and thousands of farmland acres. For the purposes of this study, only the headwaters of the Colorado River to the Colorado-Utah state line are included (Figure 17).
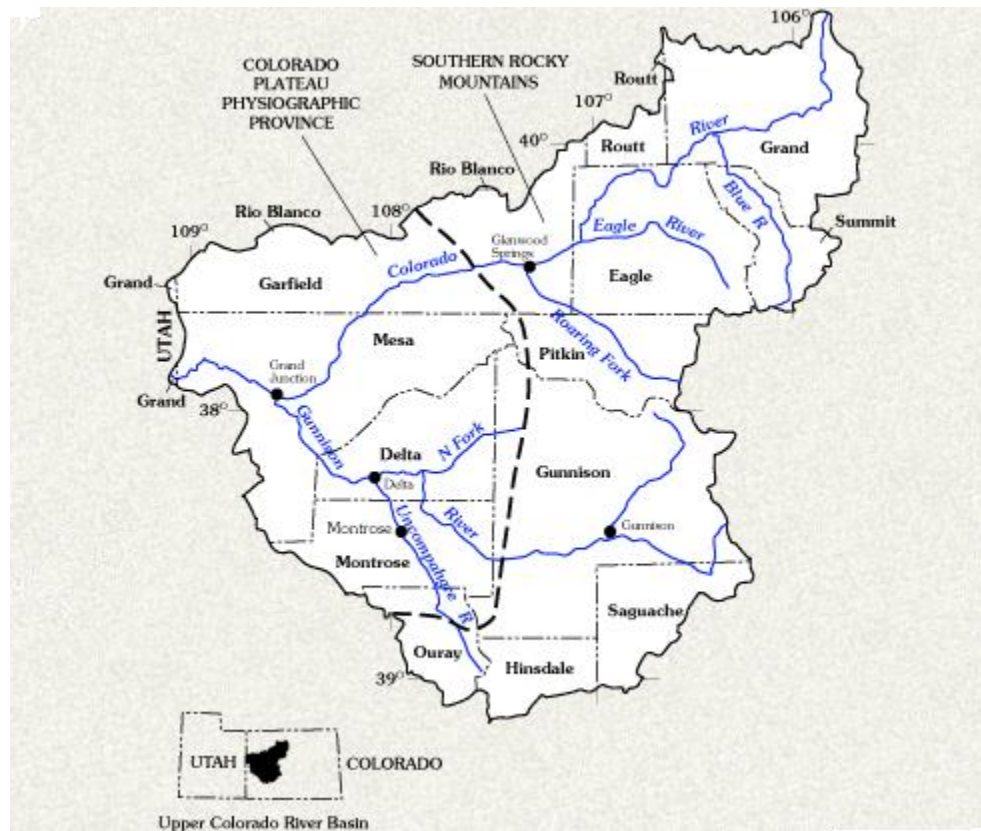
Figure 16. Map of the Upper Colorado River and significant tributaries.

This stretch of the Colorado River remains undammed—naturally flowing through the Rocky Mountains to Glenwood Springs where the Gunnison River joins at Grand Junction. The lack of storage on this portion of the river proves challenging for both long-term planning and mitigating shortages during times of need. Similar to the Gunnison River Basin, the Upper Colorado River is fed by snowfall run-off. Dominate consumptive water uses include agriculture, municipal, and transbasin diversions. Figure 17 illustrates basin's cumulative yearly surface water diversions in acre-feet by sector for 1999-2004 [*CWCB*, 2012].
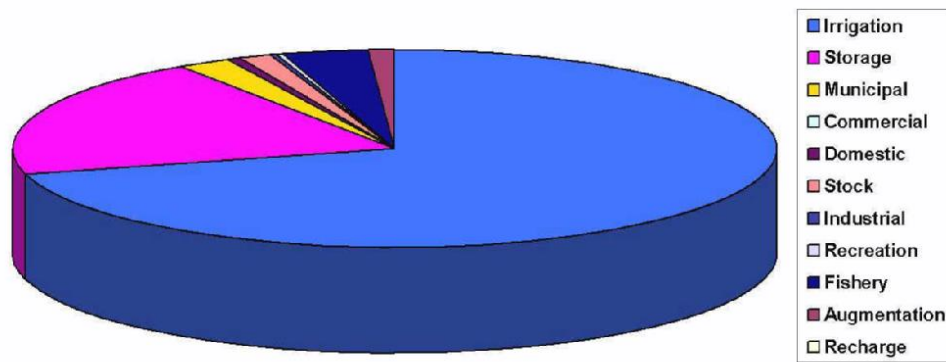
Figure 17. Pie chart of the cumulative yearly surface water diversions (acre-feet) by use provided by the Colorado Water Conservation Board (2006).

As illustrated in Figure 17, irrigation (especially in the lower Grand Valley) accounts for the majority of the surface water diversions in the Colorado River basin, followed by transbasin and off-channel storage, and municipal and industrial use. Transbasin exports account for more than 470,000 acre-feet per year [*CWCB*, 2006].

In addition to consumptive water uses (i.e., agricultural, municipal and industrial, and transbasin diversions), nonconsumptive uses are important throughout the basin. As of 2010, there were more than 400 decreed instream flow rights throughout the Colorado River basin [*CWCB*, 2011].Similarly, the Shoshone power plant holds a nonconsumptive senior water right decreeing 1,250 cubic feet per second [*Bureau of Reclamation*, 2012]. Due to the inherent nature of the water uses, some of the nonconsumptive water uses compete with the high consumptive demands—proving challenging for water resource management.

3.4 Water Management Challenges and Options for the Upper Colorado and Gunnison River Basins

The water issues present in the Upper Colorado River and the Gunnison River Basin reflect water management challenges prevalent in much of Colorado and the Colorado River Basin. These challenges include transbasin diversions, ecosystem sustainability, maintaining necessary flows to support thriving tourism and recreation industries, fulfilling water right allocations, and meeting downstream demands in light of projected population growth. Over the last decade (2000-2010), Colorado experienced rapid population growth, with much of the growth occurring in counties dependent on Upper Colorado and Gunnison River Basin water (including the Front Range). These trends are illustrated in Figure 18.
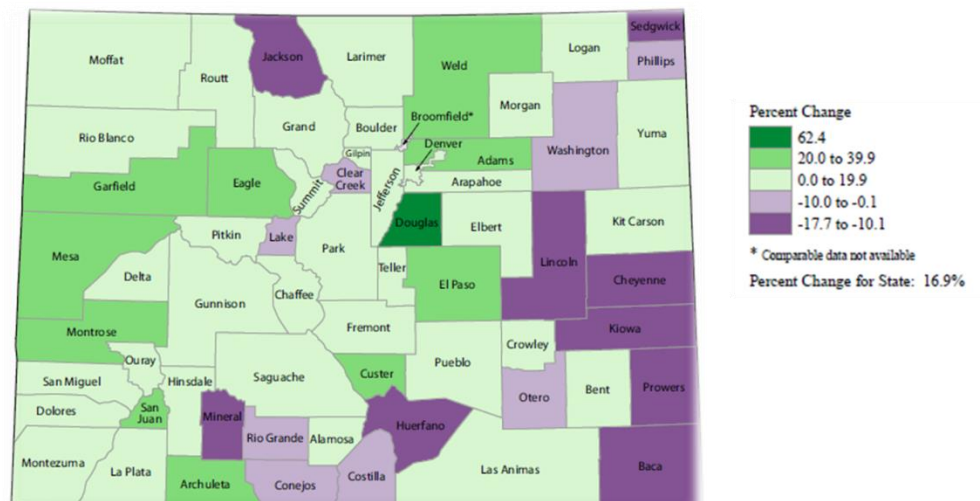
Figure 18. Population growth in Colorado from 2000-2010, provided by the U.S. Census Bureau.

Further, if population growth and development patterns continue along recent trends, the consumptive water use in the Upper Colorado and Gunnison River Basins are projected to increase more than 20% by 2060, with much of this increase occurring on the Upper Colorado River where storage is essentially nonexistent. Table 1 outlines the details of the projected growth [*Bureau of Reclamation*, 2012].

Units are thousand acre-feet per year, unless otherwise noted

Planning Area	Colorado River			Gunnison		
Hydrologic Basin Year	2015	2035	2060	2015	2035	2060
Agricultural Irrigated Acreage [thousands]	270	270	270	269	269	269
Per-Acre Water Delivery (Diversion) [af/ac/yr]	6.85	6.85	6.85	6.89	6.89	6.89
Consumptive factor [%]	26%	26%	26%	26%	26%	26%
Demand (Consumptive)	485	485	485	490	490	490
Municipal and Industrial (M&I) Population [thousands]	357	558	836	121	184	244
M&I Per Capita Use (Diversion) [gpcd]	181	173	164	173	166	157
Consumptive factor [%]	35%	35%	35%	35%	35%	35%
M&I Demand (Consumptive)	25	38	54	8	12	15
Self Served Industrial Demand (Consumptive)	3	5	5	0	1	1
Demand (Consumptive)	29	43	58	9	13	16
Energy **Demand (Consumptive)**	2	30	65	0	0	0
Minerals **Demand (Consumptive)**	10	18	19	5	9	9
Fish, Wildlife, and Recreation **Demand (Consumptive)**	0	0	0	0	0	0
Tribal **Demand (Consumptive)**	0	0	0	0	0	0
Total Hydrologic Basin **Demand (Consumptive)**	525	575	626	503	512	515

Table 1. Projected demands (2015-2061) for the Upper Colorado and Gunnison Basins provided by U.S. Bureau of Reclamation, 2012.

In light of the projected demands and the uncertainty associated with a changing climate, managing resources to mitigate shortages and avoid over-investment proves more and more challenging. As one possible solution, water managers could implement static management strategies—such as water reuse—that go into effect once vulnerability (i.e., shortage) is detected. However, decisions such as these have lasting impacts on system infrastructure, operations and budget. While they may ameliorate short-term vulnerabilities, long term they may prove both unnecessary and inefficient.

Alternatively, water managers could implement dynamic and flexible management strategies that adapt to changing climate conditions. These types of strategies move away from traditional infrastructure-based engineering approaches by focusing more on both flexibility and adaptability. Once implemented, these types of strategies can be easily adjusted—consequently improving water manager's ability to cope and minimizing regret. These types of strategies yield

benefits regardless of the climate conditions and they contain an element of flexibility, thus allowing for future adaptation [*Wilby and Dessai*, 2010]. Examples of such strategies include conservation and operational changes.

To help improve the decision-making process, the following described framework integrates decadal scale streamflow projections into a robust decision-making framework, allowing for more dynamic and efficient resource management.

3.5 Robust Decision-Making Framework

Following bottom-up approaches, the decision-making framework begins with a vulnerability analysis which helps identify which climate conditions push the system into vulnerable states and how different management strategies ameliorate these vulnerabilities. The vulnerability analysis begins with identifying system vulnerabilities and performance metrics. Once this is completed, decadal-scale, wavelet-based climate projections are generated at annual timesteps. These projections account for the current state of the natural variability cycles, and based on those, project plausible future conditions that could occur over the next decade. Using this information, relationships between system vulnerabilities and decadal-scale climate information are derived. This information is then used to develop dynamic and flexible management strategies that ameliorate system vulnerabilities. The robustness (i.e., the ability to perform well over a range of possible climate conditions) of the methodology is tested by applying the framework to a range of widely diverse plausible hydrologic future scenarios.

We intend that with this integrated process, decision-makers can implement management strategies that can be dynamically adjusted and tuned according to varying climate conditions—thus avoiding large-scale infrastructure projects that may not be needed in the long-term. An in-depth description of the methodology is presented below.

3.6 Methodology

3.6.1 Identifying System Vulnerabilities and Performance Metrics

The decision-making framework begins with the identification of system vulnerabilities and performance metrics. This process involves stakeholder collaboration to identify thresholds for performance metrics that, when violated, cause the system to be vulnerable and signify the need for adaptive management. Some thresholds may be derived from legal compacts or water rights agreements; for example, the minimum flow required to fulfill instream rights or the minimum amount of total power generated from hydroelectric reservoirs. Other thresholds and performance metrics could be physical constraints of the system, such as a maximum flood control channel capacity. In other cases, thresholds and performance metrics could be stakeholder-defined. For example, minimum flows to support threatened and endangered species, minimum reservoir pool elevations required for recreational purposes, or 95% reliability of water supply delivery.

For the Upper Colorado River and Gunnison River Basins, the selected performance metrics align with basin operations and goals, as well as water uses within the basin (previously described). The selected performance metrics span four overarching categories: ecological flows, recreation, electricity and water delivery. The thresholds were derived from historical data, calculated based on logic from the Basin Study, or taken directly from the Basin Study (which had extensive stakeholder involvement). While the thresholds are intended to be as realistic as possible, this is an illustrative example developed to demonstrate the utility of this decision-making framework and should be considered solely within this context.

Table 2 identifies the resource categories, performance metrics and vulnerability thresholds used throughout the case study.

Performance Metric	Vulnerability Threshold
Water Delivery (Resource Category)	
Basin Shortage (X)* None Low Medium High	X < 5% Depletion Requested 5% Depletion Requested ≤ X < 15% Depletion Requested 15% Depletion Requested ≤ X < 25% Depletion Requested X ≥ 25% Depletion Requested
Electric Power Resources	
Total Power Generated**	< 583,644 MWH per year for 3 consecutive years
Recreation Resources	
Shoreline Public Use Facility (Blue Mesa Pool Elevation)	≤ 7,433 feet msl
Ecological	
Gunnison River below Crystal Reservoir	< 300 cfs
*Derived from logic implemented in the Basin Study. Basin shortages are calculated separately for the Gunnison River Basin and Upper Colorado River Basin ** Derived from historical data provide by the Western Area Power Administration (WAPA)	

Table 2. System performance metrics and vulnerability thresholds.

Note, some of these performance metrics have competing objectives. For example, power generation competes with reducing shortages as management strategies focused on reducing shortage vulnerabilities inherently reduce water demands, thus requiring less water to be released from hydropower reservoirs, and, consequently, adversely impacting power generation. The instream flow right located at the gage below Crystal reservoir also competes with minimizing shortages, as instream flow rights require specific reservoir releases—which could be reduced my implementing strategies that reduce water demands. Similarly, maintaining Blue Mesa's pool

elevation competes with power generation by reducing reservoir releases, but aligns with minimizing shortages (i.e., reducing water demands and the associated reservoir releases) by keeping more water in storage. This is important to keep in mind when designing management options and strategies that alleviate system vulnerabilities.

Because performance metrics measure system performance they must be quantifiable. Given this requirement, a simulation model of the Upper Colorado and Gunnison River Basins was created in RiverWare, a generalized river basin modeling tool widely used to model river basin operations [*Zagona et al.,* 2001]. RiverWare enables users to model physical river basin features (e.g., river, reservoirs, diversions, canals, water users, and power generators) as objects. The operation of these objects is expressed as set of prioritized, logical rules written in RiverWare's unique policy language (RPL). The rule-based RiverWare simulation thus reflects operational and management strategies implemented by water managers. The Upper Colorado and Gunnison River Basin model was developed directly from the Bureau of Reclamation's long-term planning model, the Colorado River Simulation System (CRSS).

Similar to the CRSS, the Upper Colorado and Gunnison River Basin model simulates the operation of major reservoirs (i.e., the Aspinall Unit) and provides information about key output variables such as amount of storage water, reservoir elevations, dam releases, hydropower generation, water quantity at specific gages, water user diversions and return flows. While the model does not include water rights allocation, the operational logic incorporates two prominent senior water right holders on the Upper Colorado mainstem: the Shoshone Power Plant and the senior users from the Grand Valley Irrigation Company. In the model, these senior water right holders are fulfilled by shorting upstream users. For example, the operational logic ensures the Shoshone Power Plant has access to 1,250 cubic feet of water per second by shorting upstream

users. Similarly, all of the users above the Grand Valley Irrigation Company (except for Shoshone Power Plant) are shorted to ensure the senior demands are met.

A schematic of the model highlighting the selected performance metrics is presented in Figure 19.
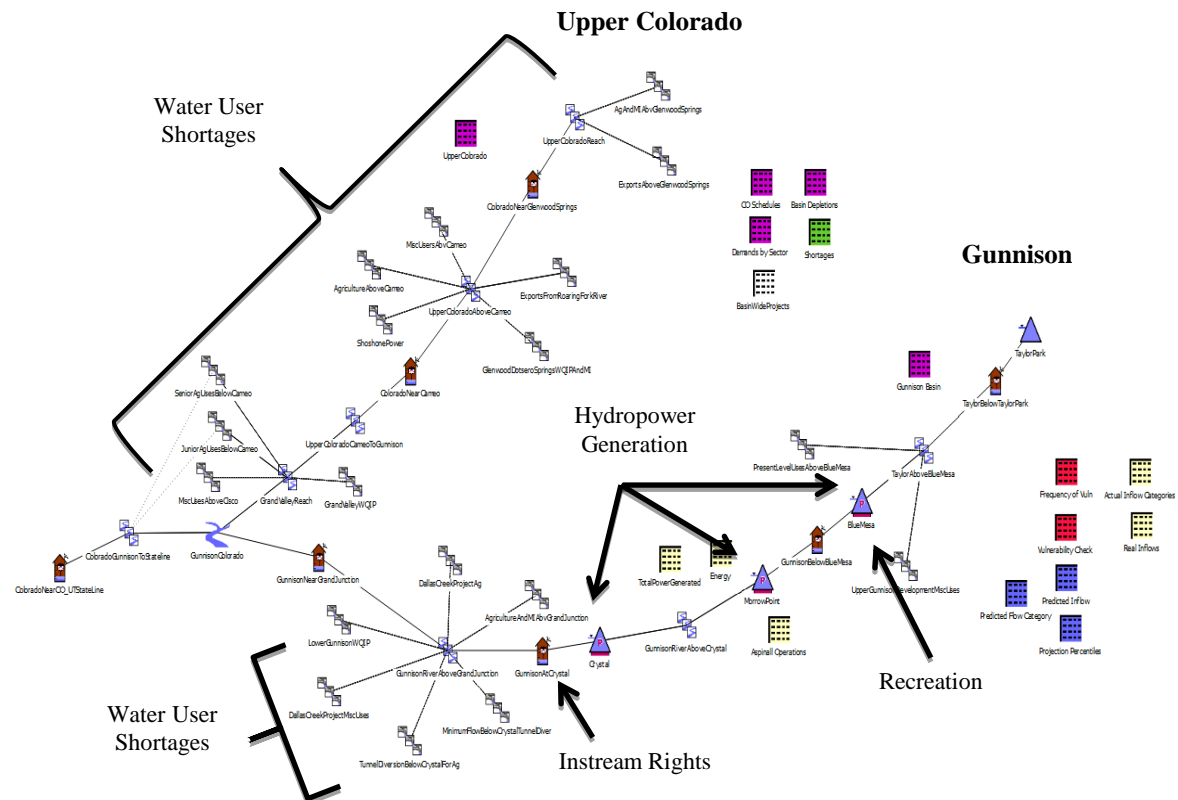
Figure 19. Schematic of the simulation model for the Gunnison and Upper Colorado River Basins developed in RiverWare.

In addition to RiverWare, our case study utilizes the RiverSMART suite of software developed under the Bureau of Reclamation's WaterSMART initiative. Built around the RiverWare modeling environment, these tools enable us to develop and import complex demand schedules, and spatially and temporally disaggregated streamflow, which can easily be imported into the RiverWare model to allow for efficient post-processing of the output variables.

In the following step, wavelet-based projections are generated at the annual timestep. Eventually, information from these projections is used to better understand system performance and vulnerability—allowing for the development of more flexible and dynamic management strategies.

3.6.2 Integrating Decadal-Scale Projections

If water managers have an enhanced understanding of plausible future hydrologic conditions occurring over the next decade, they can use this information to inform decision-making logic. Given this as the primary goal of the framework, the framework integrates decadal-scale projections generated using the wavelet-based methodology presented in Chapter 2. A brief overview of the projection methodology integrated into the decision-making framework is given below.

As previously discussed, using a historic or paleo streamflow record, wavelet analysis can be used to identify statistically significant spectral peaks which represent various natural variability cycles occurring throughout time. The natural variability cycles, at any annual timestep, can be characterized by two distinct properties: the scale average wavelet power (SAWP) and phase angle. Using the respective SAWP and phase angle, a KNN algorithm can be implemented to resample each of the filtered band passed time series—or natural variability cycles—100 times. The resampled bands are then aggregated with a modeled residual noise band to create 100 hydrologic streamflow projections. The projections span ten years in length, resulting in decadal hydrologic streamflows. By using this methodology, these projections take into account the current state of the natural variability cycles, and use this information to project possible ways the future may unfold given a historic or paleo streamflow record.

In the decision-making framework, this projection methodology is applied at every annual timestep to create decadal streamflow projections that can then be used to inform the decision-making logic. The idea being, water managers and decision makers do not know how the future will unfold; however by applying the aforementioned projection methodology at the current timestep t, decadal streamflow projections can be created. Inherent to the methodology, these projections are based on the natural variability cycles of the current timestep t—giving water managers and decision-makers improved insight into plausible future hydrologic streamflow conditions. Information from these projections is then used to inform the decision-making logic. One year passes and the water managers find themselves in the same position: not knowing how the future unfolds. However, using the observed streamflow for the previous year the historic record can be updated to include this data. Using the updated streamflow record, water manager can re-apply the projection methodology—now generating decadal-scale streamflow projections that account for the current state of the natural variability cycles. Again, water managers use the projections to inform the decision-making logic. A schematic of this concept is illustrated in Figure 20.
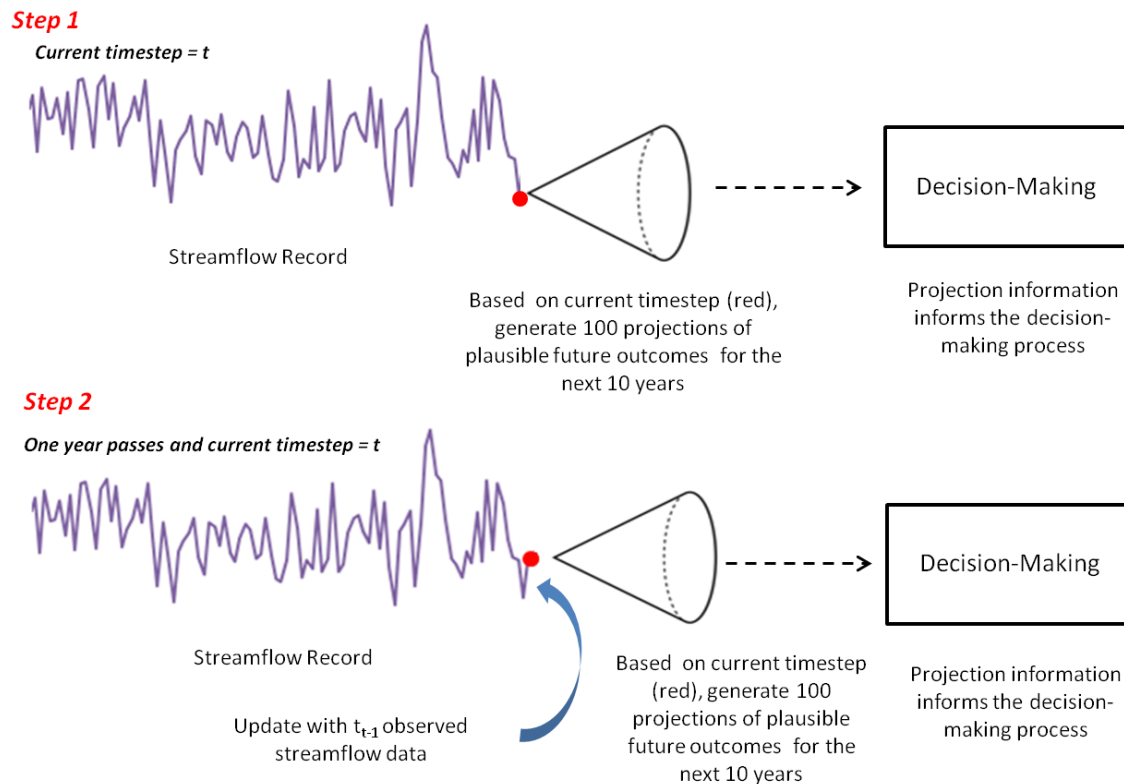
Figure 20. Schematic illustrating the generation of decadal-scale streamflow projections at annual timesteps.

This portion of the framework incorporates continuous learning by providing water managers and decision makers with decadal-scale streamflow projections that account for the current state of the natural variability cycles. These projections can then be used to inform decision-making logic—which is rooted in the most up-to-date information regarding the state of the natural variability cycles.

For the case study, the projection methodology was applied to the Lees Ferry, AZ extended paleo and historic streamflow record (1490-2010). The projections were spatially disaggregated to the seven natural inflow flow sites in the Upper Colorado and Gunnison basins per the methodology presented in *Nowak et al.* (2010). It is important to note previous research [*Nowak et al.*, 2012] identified larger scale climate indicators—specifically the Atlantic Multidecadal

Oscillation and the Pacific Decadal Oscillation—as prominent drivers of hyroclimatic variability in the Colorado River Basin. Using wavelet analysis, these larger scale climate indicators have also been identified as statistically significant spectral peaks [*Nowak et al.*, 2011]. This is important as an improved understanding of the hydrologic impacts of larger scale climate indicators coupled with the aforementioned projection methodology could be used to better inform water managers about future hydrologic conditions.

3.6.3 Deriving Relationships between Decadal Projections and System Performance

To inform the decision-making logic, relationships between the decadal-scale projections and system performance were derived. Initially, we envisioned using probability distributions of the projections to inform the decision-making logic. Per this methodology, at every annual timestep when the 100 projections were generated, a non-parametric probability distribution function (PDF) of the projections was fitted and was compared to the probability distribution of the historical streamflows. Relative to the historical terciles, we could see how the projected PDF shifted, and use this information to inform the decision-making process. For example, if there was a 65% chance of being in the lower tercile—indicating a high probability of low flow over the next ten years—we could implement strategy A. Alternatively, a 65% chance of being in the upper tercile would signify high flow years, and would require alternative action. Figure 21 highlights two PDFs created from the projection methodology.
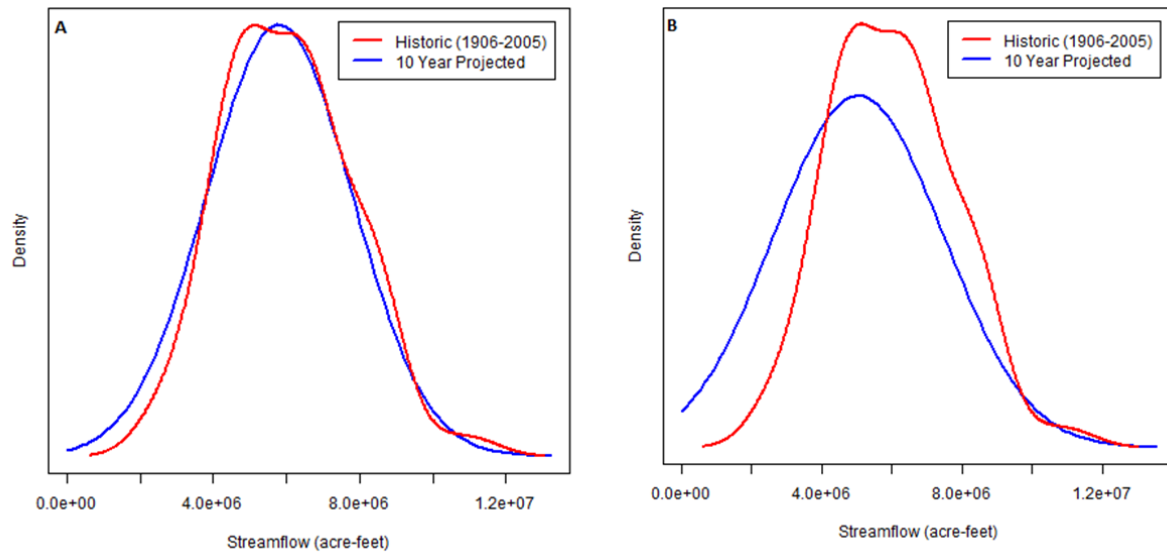
Figure 21. (A) PDF of the historic record compared to the decadal projections created at t=2012. (B) PDF of the historic record compared to the decadal projections created at t=2040.

Although there is a slight shift in Figure 21B, overall, there were not significant enough shifts in the PDFs to draw conclusions that would be informative enough for the decision-making logic. The shift in Figure 21B represents the most dramatic shifts observed for the generated projections used in the case study—making it difficult to utilize the probabilistic information.

As an alternative approach, we analyzed the performance metrics in relation to the sum of the 10 year inflows given by the projections (i.e., each projection spanning 10 years in length was summed to create a 10 year inflow). Because the model currently operates to meet water user demands, priority was given to basin shortages. A scatter plot of the sum of the basin shortages over 10 years compared to the sum of the 10 year inflow shows there is a relationship between these two parameters (Figure 22).
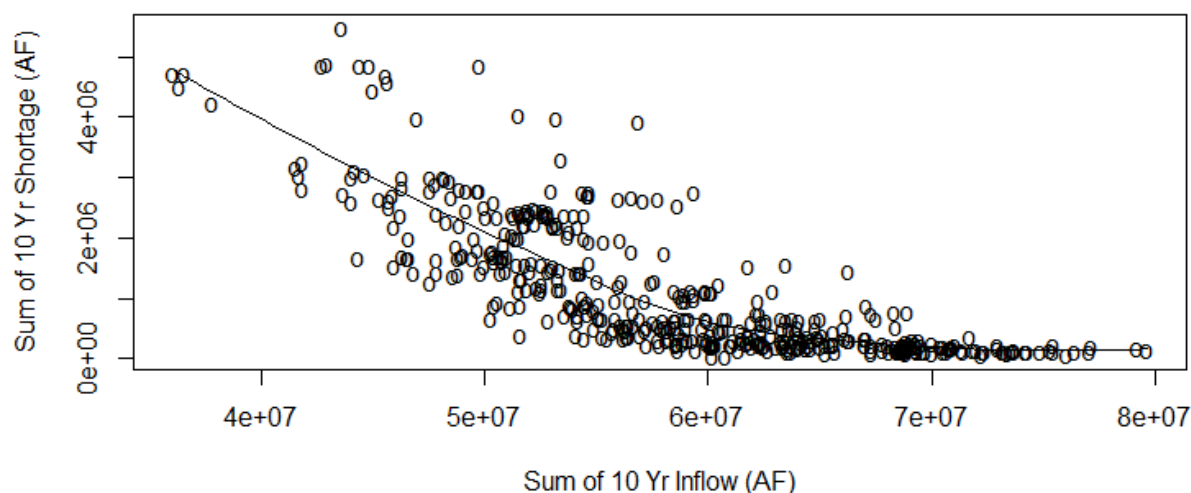
Figure 22. Scatterplot of the sum of the 10 year inflow compared to the sum of the 10 year shortage overlaid with a local polynomial.

Overlaid with a local polynomial, we see a nonlinear relationship between these two variables (Figure 22). For example, once the sum of the 10 year inflow exceeds 60,000,000 acre-feet, basin shortages remain relatively small. However, a sum of the 10 year inflow less than 60,000,000 acre-feet results in a linear relationship between the basin shortages. Thus, as inflow decreases, shortages increase.

Because the sum of the 10 year inflow can be derived from the decadal projections, a link between the projections and the primary system goal is created, achieving both water user demands and minimized basin shortages. To better understand where the shortages were geographically occurring and the flow conditions under which they were occurring, the 10 year inflow and the basin shortages were subdivided into finer resolution categories. For example, shortages were subdivided into two categories: Upper Colorado shortages, and Gunnison shortages; while the sum of the 10 year inflow was divided into nine categories (Table 3).

∑ 10 Year Inflow (*Y*, MAF)	Category
Y < 40	0
$40 \leq Y < 45$	1
$45 \leq Y < 50$	2
$50 \leq Y < 55$	3
$55 \leq Y < 60$	4
$60 \leq Y < 65$	5
$65 \leq Y < 70$	6
$70 \leq Y < 75$	7
$75 \leq Y$	8

Table 3. Selected ten year inflow thresholds and the corresponding categories.

The frequency of vulnerability for each category was then analyzed to better understand how regularly the shortages were occurring under certain inflow categories.

For this analysis, vulnerability was based on the thresholds presented in Table 2, and computed at the annual timestep. The analysis did not consider the annual frequency for the system reaching vulnerability, but rather whether the system became vulnerable in any given year. The frequency of a shortage vulnerability occurring on the Gunnison and Upper Colorado Rivers over a moving 10 year period was computed (Table 4).

A: Gunnison Basin: Frequency of Vulnerability					
∑10 Year Inflow Category	*Type of Basin Shortage (% Occurrence)*				Total Shortage
	None	Low	Med	High	
0	13	40	8	40	88
1	43	15	17	26	57
2	59	11	13	18	41
3	76	7	5	12	24
4	87	6	2	5	13
5	96	2	1	1	4
6	99	1	1	0	1
7	100	0	0	0	0
8	100	0	0	0	0

B: Upper Colorado Basin: Frequency of Vulnerability					
∑10 Year Inflow Category	*Type of Basin Shortage (% Occurrence)*				Total Shortage
	None	Low	Med	High	
0	30	40	0	30	70
1	49	23	4	23	51
2	56	24	4	17	44
3	69	17	3	11	31
4	80	14	2	5	20
5	90	6	2	2	10
6	94	4	1	1	6
7	97	3	0	0	3
8	94	6	0	0	6

Table 4. (A) A moving ten year frequency of vulnerability for the Gunnison Basin (B) moving ten year frequency of shortage vulnerability for the Upper Colorado Basin.

An example from Table 4 shows us that for an inflow category equal to zero and over a ten year moving period, there was a shortage in the Gunnison River Basin 88 percent of the time. Of that shortage, 40 percent of the time the shortage was classified as a low shortage, 8 percent as a medium shortage and 40 percent as a high shortage (see Table 1 for shortage definitions).

Analysis on this data was taken one step further to identify how the shortages impacted different sectors—specifically municipal and industrial (M&I), and agriculture (AG). Table 5 highlights these results.

∑10 Year Inflow Category	Gunnison Basin		Upper Colorado Basin	
	% M&I	% AG	% M&I	% AG
0	1	96	43	51
1	1	97	41	54
2	1	99	40	55
3	1	99	44	51
4	27	73	46	48
5	20	80	45	49
6	66	34	52	41
7	0	0	55	39
8	0	0	60	32

Table 5. Given a ten year inflow, the percent of shortage due to M&I and AG for the Upper Colorado and Gunnison Basins.

Linking the primary objective of the basin to decadal-scale information aids in the decision-making process because this information can be directly integrated into decision logic. The fundamental objective of this step is linking decadal-scale information to system performance, and drawing conclusions that can inform the decision-making process. If water managers have the ability to better understand basin inflows (provided by the projections) and how these inflows impact performance metrics (i.e. shortages) over the next 10 years, strategies targeting specific vulnerabilities can be developed and successfully implemented.

3.6.4 Identifying Flexible Management Options and Strategies that Ameliorate System Vulnerability

With improved understanding of plausible future conditions and the associated impacts on system performance, the proposed framework helps integrate this information in order to develop policies that mitigate specific vulnerabilities. Furthermore, the integration of this information provides a basis for continued learning, which helps water managers develop dynamic strategies that can adapt over time with climate change. This approach implies a new way of thinking about resource management, as it moves away from traditional management strategies focused on development and maintenance of large-scale infrastructure—which, with updated knowledge, may even prove unnecessary.

For the Gunnison and Upper Colorado case study, the relationships derived from the projections and performance metrics were used to develop adaptive management strategies that aligned with the primary objective of the basin operations, namely increasing supply reliability. In a more realistic case, water managers could develop strategies that balance the tradeoffs associated with competing objectives and performance metrics (e.g., reducing basin shortage and maintaining instream flows); however, optimization is beyond the scope of this research.

With flexible and dynamic management in mind, two types of strategies—focused on supply reliability—were developed: both M&I conservation and AG conservation. These options are feasible to implement and do not require the development of heavy infrastructure. Furthermore, the strategies can be amped up or down—depending on the information gleaned from the decadal-scale projections. For example, if water managers postulate that low flow is likely over the next ten years, they can push conservation approaches, while higher flow years would result in more normal operations (i.e., reducing conservation measures).

The results from section 3.3 further highlight the need for options and strategies that not only consider the magnitude of decadal inflow but also consider where the shortages are occurring

55

geographically given a predicted inflow, and what usage sectors contribute most to the overall shortage. By integrating all of this information together, the foundation for the conservation strategies was developed: For a given predicted 10 year inflow category (0-8), reduce the M&I user depletion requested by X% and the AG user depletion requested by Y%.

The percent reductions were derived from the data presented in Table 4 and 5, with the overarching goal of increasing system reliability. Table 6 identifies the percent reductions implemented in the study.

$\sum 10$ Year Inflow Category	Gunnison Basin		Upper Colorado Basin	
	M&I (% Reduction)	AG (% Reduction)	M&I (% Reduction)	AG (% Reduction)
0	2	10	4	6
1	2	8	4	5
2	2	6	4	5
3	1	5	3	4
4	1	2	3	3
5	0	0	2	2
6	0	0	0	0
7	0	0	0	0
8	0	0	0	0

Table 6. Percent reductions for each sector and basin implemented in the decision logic.

Again, optimization could be used to fine tune the amount that needs to be conserved (i.e., percent reduction) for optimal performance. However, given the scope of this work, the conservation logic effectively accounts for the predicted inflow category and where the shortages will most likely occur—resulting in more dynamic and adaptive management capability. Note, implementing water reuse would have similar impacts on reducing M&I shortages, however the strategy is static in that water managers can not adjust it based on new information—likely resulting in over-investment and negating the overarching goal of this framework.

The robustness of the framework is testing by applying the decision-making framework to a wide range of plausible future hydrologic scenarios. The method for choosing such scenarios is described below.

3.6.5 Generation and Selection of Plausible Future Conditions

To generate a wide range of plausible future outcomes, a set of 1500 hydrologic traces were created using three methods: a KNN resampling of the observed historical record, the wavelet-based decadal projection methodology, and the wavelet-based climate change projection methodology (Chapter 2). The KNN resampling of the observed historical record is a standard lag-1 KNN resampling method—thus it assumes history repeats itself [*U.S. Bureau of Reclamation*, 2012]. This methodology is commonly used by the Bureau of Reclamation and is comparable to the Index Sequential Method [*U.S. Bureau of Reclamation*, 2012]. Of the 1500 traces, 500 were created using the standard KNN resampling methodology. Each methodology was used to create 500 traces. For an in-depth description of the two wavelet-based projection methodologies, the reader is referred back to Chapter 2.

Note, for the Upper Colorado and Gunnison Basin streamflows, the wavelet-based decadal and climate change projections were created using the streamflow record at Lees Ferry, AZ. These projections were ultimately spatially and temporally disaggregated to the seven inflow sites represented in the simulation model per the methodology described in *Nowak et al.* (2010). While many different stochastic methods could be used to define the range of plausible future scenarios, it is important that these realizations contain the quasi-periodic natural variability components, as these have the ability to inform the decision-making process.

For computational ease, 1 percent [n=15] of the plausible future outcomes were selected. Each outcome was treated as plausible hydrologic scenario ("scenario"), in which each scenario accurately defines how the future may unfold. The 15 scenarios were selected such that they adequately cover the range of plausible future outcomes defined by the 1500 realizations. The justification for this selection is that we do not know how the future unfolds; however, we can identify specific ways in which the future unfolds, and, combined together, the realizations span the range of plausible future outcomes.

To visually depict the range of plausible future outcomes, two scatter plots of the 1500 realizations were created. Using these plots, 1 percent of the traces were hand selected such that the scope of each plot was adequately covered. The right plot compares the maximum and minimum streamflow values of the 1500 realizations (Figure 23A), while the second plot compares mean and variance of the realizations (Figure 23B).
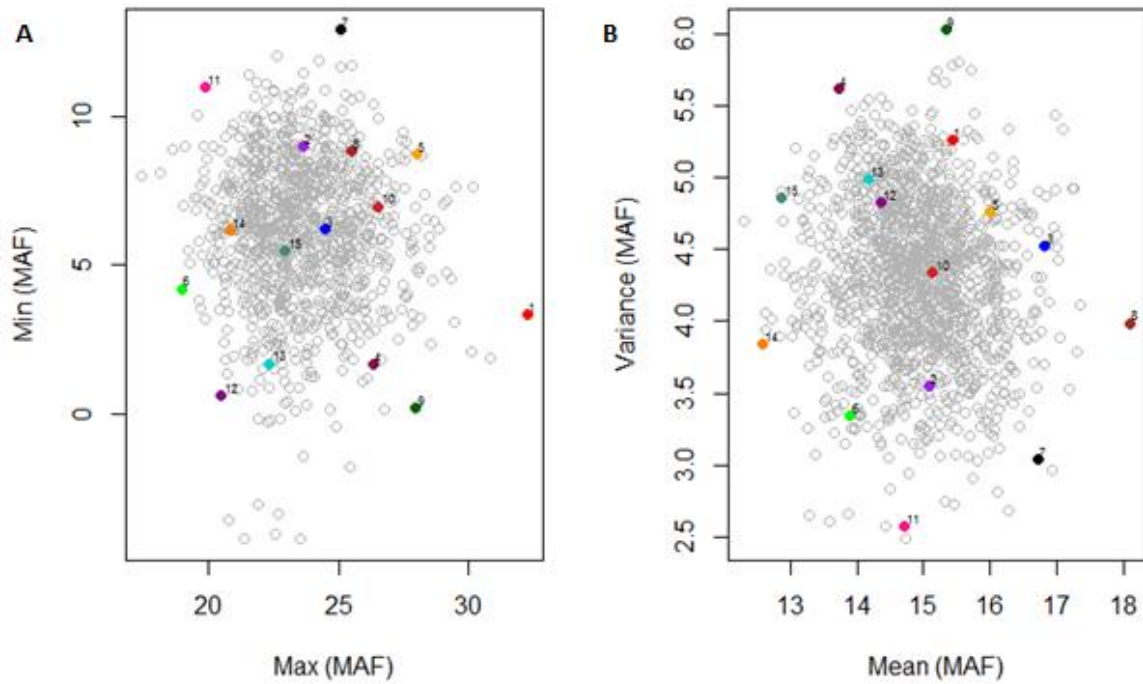
Figure 23. The 15 scenarios show in color, while the light gray represents the 1500 simulations. (A) Maximum and minimum of each trace, and (B) the mean and variance of each trace.

A histogram of the 1500 simulations compared to a histogram of the hand selected scenarios illustrates the scenarios adequately capture the overall distribution of the 1500 plausible future conditions.
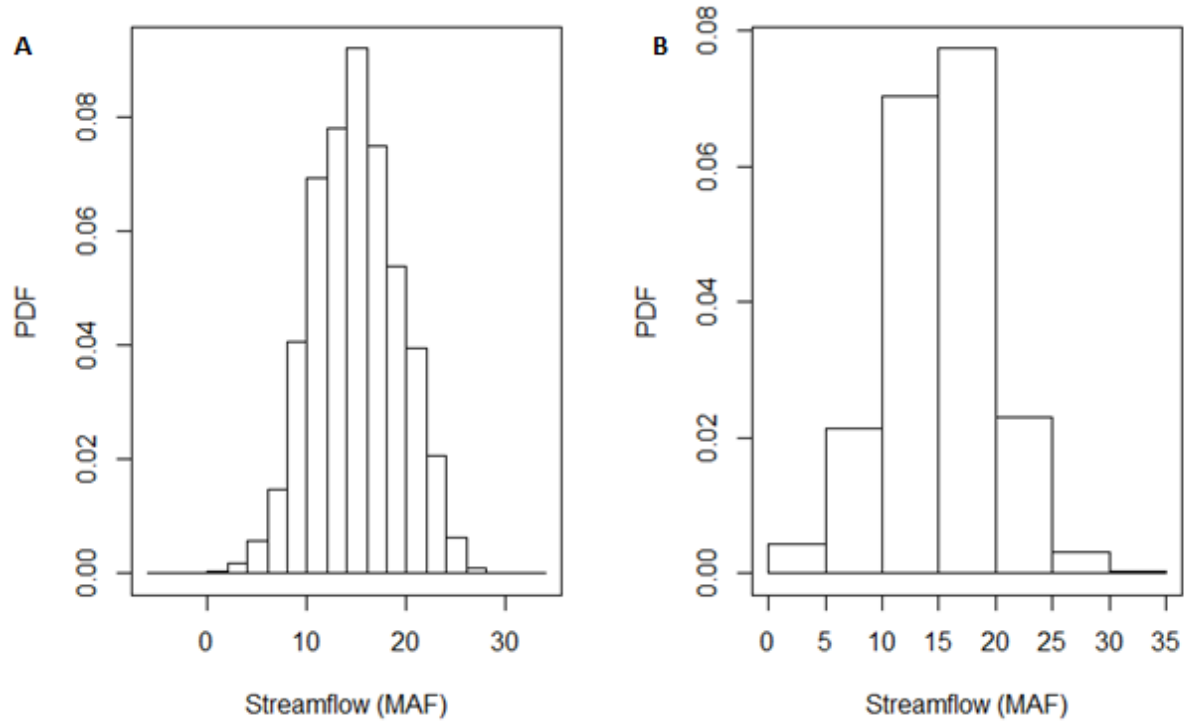
Figure 24. (A) Histogram of the 1500 simulations compared to (B) a histogram of the 15 selected scenarios.

Furthermore, Figure 25 highlights the selected scenarios (red) relative to the 1500 simulations (grey).
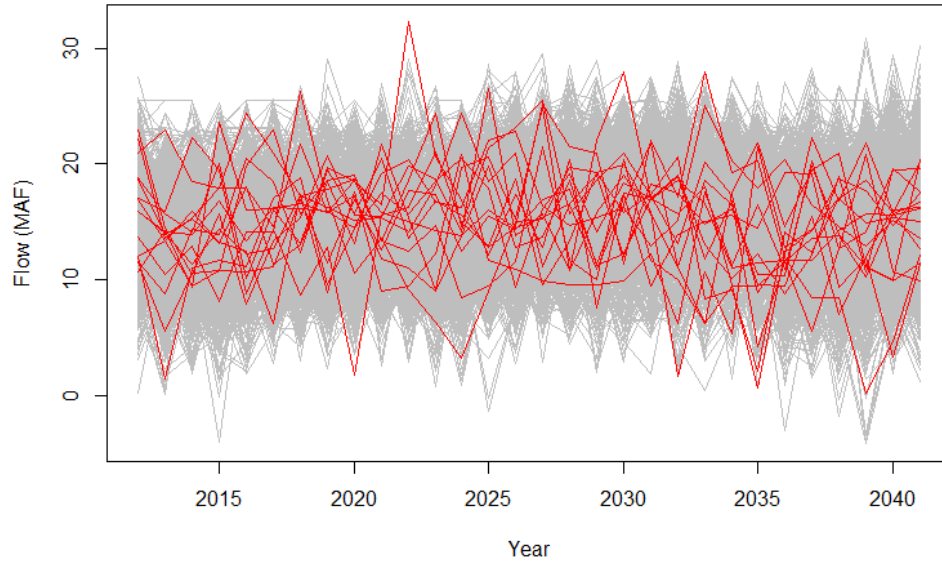
Figure 25. Selected scenarios (red) compared to the 1500 plausible future conditions (gray).

Combined together, Figures 23-25 demonstrate the proposed method for selecting the scenarios adequately covers the wide range of plausible future conditions. With this method, the maximum and minimums, as well as the mean and variance are properly addressed. For more robust coverage, more scenarios could be selected; however, with adequate coverage a larger sample size may prove unnecessary.

For the case study, the aforementioned decision-making framework was applied to each scenario. The model was simulated using the state's current demand projections (provided by the Bureau of Reclamation). Note, if the scenario originated from the wavelet-based climate change method, the projections were scaled accordingly. The results of applying the decision-making framework to the case study are presented in Chapter 4.

61

CHAPTER 4: CASE STUDY DISCUSSION AND RESULTS

This chapter contains results of applying the decision-making framework to the case study logic presented in Chapter 3. To better understand the utility and effectiveness of the proposed framework, three unique decision-logics were simulated and analyzed. The first decision-logic, called the "No Options" logic, is used as the baseline logic; it represents system performance if no management options and strategies are implemented. The second decision-logic, called the "Decadal" logic, uses the decadal projections as described in Chapter 2 to drive the decision-making logic developed in Chapter 3. The last decision-logic, "Climatology", uses the same logic as the Decadal Logic; however, the decadal projections are computed with climatology.

For the climatology projection methodology, 100 projections were created for every annual timestep by resampling the historic streamflow record with a standard lag-1 KNN resampling algorithm. As previously mentioned, this resampling methodology assumes history repeats itself and does not take into consideration the current state of the natural variability cycles. The climatology projections are independent of the hydrologic scenario.

Although the RPSS indicates the decadal projections perform only slightly better than climatology (Chapter 2), a comparison of the Decadal and Climatology decision-logic highlights the impacts these differences have on the decision-making process. For all three decision-logics, the hydrologic input consisted of the 15 scenarios described in Chapter 3, with the current state projected demands [*U.S. Bureau of Reclamation*, 2012]. The study was run from January 2012 through December 2041.

To assess the accuracy of the decadal projections relative to climatology in the decision-

making context, we analyzed the percent of times the decadal projections predicted inflow categories lower than, more than, and equal to the observed ten-year inflow. This was computed by looking at the mean projected inflow category derived for each scenario and the associated projections generated at each timestep. The mean projected inflow category was then compared to the observed inflow category (i.e., for each scenario, the ten-year inflow category given at each timestep). The results are presented in Table 7.

Projections Type	(% Projections)		
	Lower than Observed	Same as Observed	More than Observed
Decadal	42	21	37
Climatology	35	18	47

Table 7. Accuracy of predicting the ten year inflow.

These results are consistent with the RPSS presented in Chapter 2. From the 15 scenarios, the decadal projections correctly predicted the observed inflow category 21% of the time, compared to climatology which correctly predicted the observed inflow category 18% of the time. Note, the decadal projections tend to predict lower flow categories, while climatology tends to predict higher inflow categories. This is important, as the inflow categories dictate the extent of conservation—where low inflow categories push conservation and high inflow categories support normal operations.

Keeping this level of accuracy in mind, the following tables (8-9) highlight the three decision-logics' ability to mitigate shortage vulnerability on both the Gunnison and Upper Colorado basins.

	Gunnison Basin Shortages										
	Number of Vulnerabilities Over 30 Years										
Scenario	No Options				Decadal & Options				Climatology & Options			
	None	Low	Medium	High	None	Low	Medium	High	None	Low	Medium	High
1	27	2	0	1	28	1	0	1	28	1	0	1
2	29	0	0	1	29	0	0	1	29	0	0	1
3	29	0	1	0	29	1	0	0	29	1	0	0
4	22	1	3	4	22	1	3	4	22	2	2	4
5	28	1	1	0	28	2	0	0	28	1	1	0
6	26	3	0	1	26	3	0	1	26	3	0	1
7	30	0	0	0	30	0	0	0	30	0	0	0
8	30	0	0	0	30	0	0	0	30	0	0	0
9	25	2	1	2	25	2	1	2	25	2	1	2
10	27	1	1	1	27	2	1	0	27	2	0	1
11	29	1	0	0	30	0	0	0	30	0	0	0
12	26	2	0	2	26	2	0	2	26	2	0	2
13	26	0	0	4	26	0	2	2	26	0	0	4
14	22	3	2	3	22	3	2	3	22	3	2	3
15	16	6	5	3	18	6	3	3	17	7	3	3
Total	392	22	14	22	396	23	12	19	395	24	9	22

Table 8. For each scenario and decision-logic, the number of vulnerabilities over the entire run period (2012-2041).

64

	Upper Colorado Basin Shortages										
	Number of Vulnerabilities Over 30 Years										
Scenario	No Options				Decadal & Options				Climatology & Options			
	None	Low	Medium	High	None	Low	Medium	High	None	Low	Medium	High
1	23	5	0	2	25	3	0	2	24	4	0	2
2	27	3	0	0	27	3	0	0	27	3	0	0
3	28	1	0	1	28	1	0	1	28	1	0	1
4	21	4	1	4	21	4	1	4	21	4	1	4
5	26	3	1	0	27	3	0	0	27	3	0	0
6	25	3	1	1	25	3	1	1	25	3	1	1
7	30	0	0	0	30	0	0	0	30	0	0	0
8	30	0	0	0	30	0	0	0	30	0	0	0
9	24	3	1	2	24	3	1	2	24	3	1	2
10	24	5	0	1	26	3	1	0	26	3	0	1
11	27	3	0	0	28	2	0	0	29	1	0	0
12	24	3	1	2	24	3	1	2	24	3	1	2
13	20	6	2	2	21	5	2	2	21	5	2	2
14	19	7	2	2	19	7	3	1	19	7	3	1
15	20	7	0	3	20	7	0	3	20	7	0	3
Total	368	53	9	20	375	47	10	18	375	47	9	19

Table 9. For each scenario and decision-logic, the number of vulnerabilities over the entire run period (2012-2041).

On the Gunnison Basin, the decadal decision-logic mitigates more vulnerability compared to climatology. Using the decadal projections and management options and strategies, the number of high shortages was reduced, resulting in an increase of medium-level shortages. This is to be expected, as the high shortages were reduced to less severe shortages (i.e., medium) through conservation. By a small margin, the decadal projections do a better job mitigating shortage vulnerability relative to climatology.

Interestingly, on the Upper Colorado Basin the decadal and climatology decision-logics perform similarly compared to the no options decision-logic. For example, both the decadal and

climatology decision-logics result in the same number of no and low shortages. However, the decadal decision-logic results in fewer high shortages. Relative to climatology, the decadal decision-logic mitigated more shortages on the Gunnison Basin compared to the Upper Colorado Basin—suggesting storage plays a key role in utilizing decadal scale information to increase supply reliability. For example, with available storage and dynamic management strategies, water managers could implement strategies that store excess water during high flow epochs, which can be used to increase supply reliability during low flow epochs. However, the lack of storage on the Upper Colorado Basin proves difficult for such planning.

Table 10 summarizes the overall impacts of each decision-logic in reducing basin-wide (i.e., Gunnison and Upper Colorado) shortages.

Combined Shortages (Number of Vulnerabilities Over 30 Years)			
Shortage	No Options	Decadal & Options	Climatology & Options
None	760	771	770
Low	75	70	71
Medium	23	22	18
High	42	37	41

Table 10. Total shortage vulnerabilities for the Upper Colorado and Gunnison Basins given all 15 scenarios.

Consistent with the previous results, the decadal decision-logic does a slightly better job mitigating shortage vulnerability compared to climatology and no options.

Both decadal and climatology decision-logic results show that the logic integrated into the framework is effective. Given that the decadal projections only perform slightly better than climatology, the framework considers a predicted ten-year inflow and responds accordingly.

Tables 11-12 provide a summary of the overall effects of the framework on both the Gunnison and Upper Colorado Basins for the 15 scenarios.

Impacts of the Framework on the Gunnison Basin		
	Decadal	Climatology
Completely Eliminated (%)	7	5
Reduced to a Lesser Type of Shortage (%)	12	7
Reduced but Not Enough to Change the Type of Shortage (%)	64	59
High (%)	46	44
Medium (%)	16	24
Low (%)	38	32
Unchanged (%)	17	29
High (%)	30	41
Medium (%)	30	12
Low (%)	40	47

Table 11. Overall impacts of the decision-logic on the Gunnison Basin.

Impacts of the Framework on the Upper Colorado		
	Decadal	**Climatology**
Completely Eliminated (%)	7	9
Reduced to a Lesser Type of Shortage (%)	0	2
Reduced but not Enough to Change Type of Shortage (%)	93	89
High (%)	24	26
Medium (%)	11	11
Low (%)	57	63
Unchanged (%)	**0**	**0**
High (%)	-	-
Medium (%)	-	-
Low (%)	**-**	**-**

Table 12. Overall impacts of the decision-logic on the Upper Colorado Basin.

Overall, on the Gunnison Basin, the decadal decision-logic eliminated more of the shortages and had a bigger impact on reducing the severity of the shortages. These results could be biased, as the decadal projections often predict the ten year inflow will be less than the observed, resulting in increased conservation measures. Similarly, the climatology decision-logic has a higher percent of not addressing the shortages—which could be a result of the climatology projections predicting the ten year inflow will be more than the observed and, consequently, resulting in less conservation.

On the Upper Colorado, the framework addressed all of the shortages—either reducing them to less severe shortages or eliminating them all together. However, as previously discussed, there is little difference between the climatology and decadal decision-logics.

Although the adaptive management strategies primarily target mitigation of shortage vulnerabilities, performance of the other metrics was quantified. Tables 13-15 show the results of individual metrics under each scenario.

Energy: Total Power Generated			
	Number of Vulnerabilities Over 30 Years		
Scenario	**No Options**	**Decadal & Options**	**Climatology & Options**
1	0	0	0
2	0	0	0
3	0	0	0
4	5	5	5
5	1	1	1
6	3	3	3
7	0	0	0
8	0	0	0
9	3	3	3
10	3	2	3
11	1	0	1
12	4	4	4
13	4	3	4
14	8	6	6
15	6	6	6
Total	**38**	**33**	**36**

Table 13. Total power generated frequency of vulnerability (2012-2041).

Recreation: Blue Mesa Pool Elevation		
	Number of Violations Over 30 Years		
Scenario	No Options	Decadal & Options	Climatology & Options
1	10	10	10
2	9	8	8
3	3	2	2
4	17	17	17
5	11	10	10
6	16	15	16
7	2	1	2
8	2	2	2
9	9	9	9
10	12	10	10
11	12	12	12
12	14	13	14
13	12	12	12
14	22	21	22
15	19	19	19
Total	170	161	165

Table 14. Blue Mesa pool elevation frequency of vulnerability (2012-2041).

Instream Right: Flow at Crystal Gage			
	Number Violations Over 30 Years		
Scenario	No Options	Decadal & Options	Climatology & Options
1	2	2	2
2	2	2	2
3	0	0	0
4	9	9	9
5	4	4	3
6	6	6	6
7	0	0	0
8	0	0	0
9	4	4	4
10	4	4	4
11	0	0	0
12	5	4	5
13	5	5	5
14	9	8	8
15	7	7	7
Total	**57**	**55**	**55**

Table 15. Instream right frequency of vulnerability at Gunnison gage below Crystal Reservoir (2012-2041).

For all performance metrics, implementing this decision-logic improved the overall performance of the system by reducing vulnerability. This underscores the utility of this type of approach and the importance of using decadal scale projections to inform flexible decision-making. Furthermore, some of these metrics inherently have competing objectives and, despite this, the options and strategies still improved overall performance. For the total power generated—a metric that competes with reducing shortages—and the Blue Mesa pool elevation, which aligns with the shortage objectives, the decadal decision-logic improved system performance slightly more than climatology. Similarly, instream rights—measured at Gunnison gage below the Crystal Reservoir—compete with the shortages objective, and yet the options and

strategies still reduce vulnerability. While not perfect, these results illustrate the benefits of employing options and strategies that adapt as climate changes.

A brief cost analysis comparing all three decision-logics is included. This is important as it highlights the costs associated with basin shortages, as well as the costs associated conservation. These costs associated with conservation could include the costs of not conserving enough (i.e., the cost of shortages), the cost of over-conserving, and the associated lost opportunity costs. Given the importance of understand all of the costs, this analysis is twofold.

The first part of the analysis quantifies the amount conserved under the decadal and climatology decision-logics when conservation is not needed (i.e., there is no shortage, yet conservation is still implemented). These results highlight the opportunity for implementing optimization to fine tune the extent the management options and strategies are implemented (Tables 16 and 17).

	Gunnison Basin						
	No Need for Conservation: Quantity Over-Conserved *(acre-feet)*						
	Decadal			**Climatology**			**Scenario Resulting in Most Over-Conservation**
Scenario	**M&I**	**AG**	**Total**	**M&I**	**AG**	**Total**	
1	10	0	10	4	0	4	Decadal
2	565	23131	23696	281	9999	10280	Decadal
3	300	6880	7179	25	5813	5837	Decadal
4	11	588	599	4	5	8	Decadal
5	10	3	13	5	6422	6427	Climatology
6	584	15471	16055	296	9422	9719	Decadal
7	22	0	22	5	3	8	Decadal
8	17	3	20	7	3	10	Decadal
9	576	17051	17626	17	3301	3319	Decadal
10	852	10562	11414	299	8016	8316	Decadal
11	575	15024	15599	11	4	14	Decadal
12	576	16147	16723	283	1822	2104	Decadal
13	315	1969	2284	12	577	589	Decadal
14	857	18005	18863	849	17344	18193	Decadal
15	4	0	3	7	0	7	Climatology

Table 16. Quantity that was over-conserved when Conservation was not needed for the Gunnison Basin.

Upper Colorado Basin						
No Need for Conservation: Quantity Over-Conserved						
(acre-feet)						
Scenario	**Decadal**			**Climatology**			**Scenario Resulting in Most Over-Conservation**
	M&I	**AG**	**Total**	**M&I**	**AG**	**Total**	
1	9892	8783	18675	10324	9191	19515	Climatology
2	16176	22705	38881	13789	21077	34866	Decadal
3	11183	9097	20280	10306	8359	18665	Decadal
4	12124	6637	18761	9153	4787	13940	Decadal
5	9846	20913	30758	7649	15994	23643	Decadal
6	15646	12456	28101	14493	11555	26048	Decadal
7	11359	17084	28443	9437	15302	24740	Decadal
8	16580	24974	41554	11572	19940	31513	Decadal
9	8530	17721	26250	9032	16210	25242	Decadal
10	12053	17424	29477	10569	17943	28512	Decadal
11	13460	26614	40074	10961	20575	31536	Decadal
12	17865	34638	52502	13856	26614	40470	Decadal
13	11673	30027	41700	6918	18090	25009	Decadal
14	12660	20074	32734	10671	23775	34447	Climatology
15	10688	35671	46359	11108	28988	40096	Decadal

Table 17. Quantity that was over-conserved when Conservation was not needed for the Upper Colorado Basin.

This analysis is performed within the context of the framework which implements management strategies to increase supply reliability. Inherently, the framework implements conservation when it may not be needed, and vice versa. For a more efficient framework, further analysis quantifying the optimal levels of implementation could be included. However, given the framework, in some hyrdrologic scenarios, climatology results in more over-conservation, while in others the decadal projections result in more over-conservation. On the Gunnison Basin, climatology results in more over-conservation on two out of the fifteen scenarios (scenario 5 and 15). Similarly, on the Upper Colorado, climatology results in more over-conservation on two out of the fifteen scenarios (scenario 1 and 14).

The second part of the cost analysis looks at when conservation is implemented, how much more needs to be implemented to eliminate shortages under each of the different decision-logics (Tables 18 and 19).

	Gunnison Basin						
	Conservation Needed: Quantity Should Have Conserved to Eliminate Shortages (acre-feet)						
	No Options		**Decadal**		**Climatology**		**Scenario that has to conserve the least to reduce shortages**
Scenario	**M&I**	**AG**	**M&I**	**AG**	**M&I**	**AG**	
1	1406	326210	1105	292930	1378	312208	Decadal
2	1000	145634	1000	145634	979	117236	Climatology
3	581	63891	257	36809	565	51664	Decadal
4	7864	1220750	7528	1163694	7468	1166424	Decadal
5	791	110363	766	66899	778	83443	Decadal
6	1928	223370	1842	188286	1916	207536	Decadal
7	-	-	-	-	-	-	-
8	-	-	-	-	-	-	-
9	11096	873505	10878	817387	11068	860387	Decadal
10	2109	218328	1200	152157	2089	209632	Decadal
11	-	7506	-	-	-	-	-
12	4746	760765	3568	694725	3967	747608	Decadal
13	5526	1032035	4577	921120	5490	1000464	Decadal
14	6616	756600	6220	702873	6173	695003	Climatology
15	8893	1048273	8217	910376	8400	987745	Decadal

Table 18. The amount that needs to be conserved to eliminate shortages on Gunnison Basin.

Upper Colorado Basin							
	Conservation Needed: Quantity Should Have Conserved to Eliminate Shortages (acre-feet)						**Scenario that has to conserve the least to reduce shortages**
Scenario	**No Options**		**Decadal**		**Climatology**		
	M&I	**AG**	**M&I**	**AG**	**M&I**	**AG**	
1	798199	884404	759887	829898	763542	826622	Decadal
2	43380	61943	34800	35521	35854	44714	Decadal
3	170313	217324	154168	186857	157423	194138	Climatology
4	1429383	2003124	1364966	1920835	1356091	1907290	Climatology
5	101001	160611	84714	135848	82980	131238	Climatology
6	475266	644669	438616	586678	453857	609407	Decadal
7	-	-	-	-	-	-	-
8	-	-	-	-	-	-	-
9	1060597	1536004	997905	1425011	1019104	1469896	Decadal
10	242714	319600	206925	255987	221095	284730	Decadal
11	48987	4658	41620	0	42024	1480	Decadal
12	1092726	1684122	1045162	1577937	1063629	1626873	Decadal
13	1158273	1691536	1082692	1543807	1107906	1608349	Decadal
14	597371	968853	542624	858965	539633	852266	Climatology
15	946122	1198188	875833	1085345	894706	1113771	Decadal

Table 19. The amount that needs to be conserved to eliminate shortages on Upper Colorado Basin.

On the Gunnison, where storage is available, the decadal decision-logic does a better job conserving, thus requiring less water to increase supply reliability. While the decadal decision-logic also perform better on the Upper Colorado basin, climatology plays a stronger role. This raises the question of the utility of the decadal projections under different hydrologic conditions and the presence of storage. It could be the decadal projections only prove more useful than climatology under prolonged dry conditions where storage is available. This could be further investigated using synthetic data as none of the selected scenarios show prolonged dry epochs in the study period (2012-2041). The dry epochs appear post 2040.

Throughout the analysis, the decadal decision-logic tends to over-conserve while the climatology decision-logic often does not conserve enough. Both of these situations have

associated costs—one resulting in inefficient use of resources while the other adversely impacts supply reliability. Ideally, with improved decadal projections, the supply reliability targets would be met more consistently—resulting in more efficient management. Nonetheless, this framework effectively demonstrates the importance of robust decision-making, how decadal scale projections can inform the decision-making process, and the importance of adaptive, flexible management.

A summary of this work is provided in Chapter 5.

CHAPTER 5: CONCLUSION

This research seeks to demonstrate the value of incorporating decadal scale information into water resource decision-making frameworks that integrate dynamic, flexible management strategies. Because previous research links decadal variability to water supply reliability—specifically in the Colorado River Basin—integrating this knowledge into decision-making frameworks is of great potential value. Currently, some decision-making frameworks use small scale climate variables (i.e., temperature and precipitation) to inform the decision-making process; however this overlooks the importance of leading hydroclimatic drivers—such as decadal variability. To this end, this research develops a methodology for creating stochastic streamflow projections based on non-stationary spectral properties. As described in Chapter 3, the methodology uses the wavelet transform to identify statistically significant variability peaks, which can be filtered to create band passed timeseries. The current state of the system is then characterized by the band's Scale Average Wavelet Power (SAWP) and phase angle. Built around this information, a KNN algorithm creates simulations each band individually, which can then be summed together to create streamflow projections. While important statistical measures were captured in this methodology (mean, variance, skew, min and max), the methodology fails to adequately capture the band's amplitude and phase—a challenge prevalent in many long-term prediction methods. Unfortunately, the methodology does not prove as skillful as we would have liked as the RPSS suggests the method produces projections that perform slightly better than climatology. Despite this shortcoming, the projections prove useful for informing decision-making processes.

In addition to developing a decadal scale projection methodology, this research develops a robust decision-making framework that integrates decadal information to inform decision logic.

The utility of this framework is presented in Chapter 3, with the results from a case study on the Gunnison and Upper Colorado River Basins presented in Chapter 4. The framework is built around the idea of incorporating large-scale climate information to drive decision-making processes—resulting in more adaptive and flexible management in light of climate change. Despite the skill of the proposed decadal projections, the framework effectively demonstrates the utility of integrating this information into decision-making.

Using this approach, the decision-logic for the case study incorporated knowledge about decadal scale inflows and system performance to target geographic and sector-based shortages. Overall, basin shortages, both on the Upper Colorado and Gunnison Rivers, were mitigated and reduced—increasing system reliability and overall system performance. These results suggest linking system performance to decadal scale variability proves useful for developing and implementing flexible management strategies. With improved projections, this framework has the potential to be even more beneficial to water managers.

For improvements, future work should focus on creating improved decadal scale projections. As mentioned in Chapter 2, the physical processes that drive decadal variability need to be better understood as well as the interactions between anthropogenic forcings and natural variability. With improved projections, future work could assess whether probabilistic information could better inform the decision-logic. Furthermore, optimization could be integrated into the framework to help identify optimal levels of management implementation—resulting in improved efficiency and balance between competing objectives.

REFERENCES

Brown, Casey (2010), Decision-scaling for Robust Planning and Policy under Climate Uncertainty, World Resources Report. Available online at http://www.worldresourcesreport.org.

Brown, C., Y.Ghile, M.Laverty, and K.Li (2012), Decision scaling: Linking bottom-up vulnerability analysis with climate projections in the water sector, Water Resour. Res., 48.

Cayan, D. R., K. T. Redmond, and L. G. Riddle (1999), ENSO and hydrologic extremes in the western United States, *Journal of Climate*, *12*, 2881-2893.

"Colorado Basin Factsheet," (2006). The Colorado Water Conservation Board. Available online at http://cwcbweblink.state.co.us/weblink/docview.aspx?id=113227&searchhandle=30039

Dessai, S., M.Hulme, R.Lempert, and R.Pielke (2009), Climate predictions: A limit to adaptation? in *Adapting to Climate Change: Thresholds, Values, Governance*, edited by N.Adger et al., Cambridge Univ. Press, Cambridge, U.K.

Gober, P., and C. W. Kirkwood (2010), Vulnerability assessment of climate-induced water shortage in Phoenix, *Proceedings of the National Academy of Sciences of the United States of America*, *107*, 21295-21299.

"Gunnison Basin Water: No Panacea for the Front Range," (2003). The Land and Water Fund of the Rockies, Colorado.

Hallegatte, S. (2009), Strategies to adapt to an uncertain climate change, *Global Environ. Change*, 19, 240–247.

Hidalgo, H. G., M. D.Dettinger, and D. R.Cayan (2008), Downscaling with constructed analogues: Daily precipitation and temperature fields over the United States, Rep. CEC-500-2007-123, Calif. Energy Comm., PIER Energy-Related Environ. Res., Sacramento, Calif.

Hidalgo, H. G., and J. A. Dracup (2003), ENSO and PDO effects on hydroclimatic variations of the Upper Colorado River basin, *Journal of Hydrometeorology*, *4*, 5-23.

Keenlyside, N. S., M. Latif, J. Jungclaus, L. Kornblueh, and E. Roeckner (2008), Advancing decadal-scale climate prediction in the North Atlantic sector, *Nature*, *453*, 84-88.

Kwon, H.-H., U. Lall, and A. F. Khalil (2007), Stochastic simulation model for nonstationary time series using an autoregressive wavelet decomposition: Applications to rainfall and temperature, *Water Resour. Res*., 43.

Lall, U., and A. Sharma (1996), A nearest neighbor bootstrap for time series resampling, *Water Resour. Res.*, 32(3), 679–693.

Lempert, R., D.Groves, S.Popper, and S.Bankes (2006), A general, analytic method for generating robust strategies and narrative scenarios, *Manage. Sci.*, 52(4), 514–528.

Lempert, R., J. and David G. Groves (2010), Identifying and evaluating robust adaptive policy responses to climate change for water management agencies in the American west, *Technological Forecasting and Social Change*, 77(6), 960-974.

McCabe, G. J., J. L. Betancourt, and H. G. Hidalgo (2007), Associations of decadal to multidecadal sea-surface temperature variability with Upper Colorado River flow, *Journal of the American Water Resources Association*, *43*, 183-192.

McCabe, G. J., and M. D. Dettinger (1999), Decadal variations in the strength of ENSO teleconnections with precipitation in the western United States, *International Journal of Climatology*, *19*, 1399-1410.

Meehl, G. A., L. Goddard, J. Murphy, R. J. Stouffer, G. Boer, G. Danabasoglu, K. Dixon, M. A. Giorgetta, A. M. Greene, E. Hawkins, G. Hegerl, D. Karoly, N. Keenlyside, M. Kimoto, B. Kirtman, A. Navarra, R. Pulwarty, D. Smith, D. Stammer, and T. Stockdale (2009), Decadal Prediction Can It Be Skillful?, *Bulletin of the American Meteorological Society*, *90*, 1467-+.

Mehta, V., G. Meehl, L. Goddard, J. Knight, A. Kumar, M. Latif, T. Lee, A. Rosati, and D. Stammer (2011), Decadal Climate Predictability and Prediction Where Are We?, *Bulletin of the American Meteorological Society*, *92*, 637-640.

Miller, A. J., D. R. Cayan, T. P. Barnett, N. E. Graham, and J. M. Oberhuber (1994), The 1976-77 Climate Shift of the Pacific Ocean, *Oceanography*, *7*, 21-26.

Nowak, K., J. Prairie, B. Rajagopalan, and U. Lall (2010), A Non-parametric Stochastic Approach for Multisite Disaggregation of Annual to Daily Streamflow, *Water Resources Research*, 46.

Nowak, Kenneth C. (2011), Stochastic Streamflow Simulation at Interdecadal Times Scales and Implications for Water Resources Management in the Colorado River Basin, Civil, Environmental, and Architectural Engineering Ph.D. Thesis, University of Colorado, Boulder, CO.

Nowak, K., B. Rajagopalan and E. Zagona (2011), Wavelet Auto-Regressive Method (WARM) for multi-site streamflow simulation of data with non-stationary spectra, *Journal of Hydrology*, 410 (1-2) 1-12.

Nowak, K., M. Hoerling, B. Rajagopalan, and E. Zagona (2012), Colorado River Basin Hydroclimatic Variability, *Journal of Climate*, 25 (2), 4389-4403.

Piechota, T. C., J. A. Dracup, and R. G. Fovell (1997), Western US streamflow and atmospheric circulation patterns during El Nino Southern Oscillation, *Journal of Hydrology*, *201*, 249-271.

"IPCC Fourth Assessment Report." (2007). IPCC, Geneva.

Rajagopalan, B., K. Nowak, J. Prairie, M. Hoerling, B. Harding, J. Barsugli, A. Ray, and B. Udall (2009), Water supply risk on the Colorado River: Can management mitigate?, *Water Resources Research*, *45*, -.

Rajagopalan, B., and U. Lall (1999), A k-nearest-neighbor simulator for daily precipitation and other weather variables, *Water Resour. Res.*, 35(10), 3089–3101.

Rajagopalan, Balaji, Michael E. Mann, Upmanu Lall, (1998), A Multivariate Frequency-Domain Approach to Long-Lead Climatic Forecasting*. *Wea. Forecasting*, 13, 58–74.

Solomon, Amy, and Coauthors (2011), Distinguishing the Roles of Natural and Anthropogenically Forced Decadal Climate Variability. *Bull. Amer. Meteor. Soc.*, 92, 141–156.

Stainforth, D. A., et al. (2007), Issues in the interpretation of climate model ensembles to inform decisions, *Philos. Trans. R. Soc. A*, 365, 2163–2177.

Tebaldi, C., R. W.Smith, D.Nychka, and L. O.Mearns (2005), Quantifying uncertainty in projections of regional climate change: A Bayesian approach to the analysis of multi-model ensembles, *J. Clim.*, 18, 1524–1540.

Timilsena, J., T. Piechota, G. Tootle, and A. Singh (2009), Associations of interdecadal/interannual climate variability and long-term colorado river basin streamflow, *Journal of Hydrology*, *365*, 289-301.

The Colorado Water Conservation Board (CWCB).Colorado. *Statewide Water Supply Initiative 2010*. 2011.

Torrence, C., and G. P. Compo (1998), A practical guide to wavelet analysis, *Bulletin of the American Meteorological Society*, *79*, 61-78

U.S. Bureau of Reclamation (2012), Colorado River Basin Water Supply and Demand Study, U.S. Dep. of Inter., Washington, D.C.

U.S. Bureau of Reclamation (2013), Colorado River Basin Natural Flow and Salt Data, U.S. Dep. of Inter., Washington, D.C.

Weaver, C. P., Lempert, R. J., Brown, C., Hall, J. A., Revell, D. and Sarewitz, D. (2013), Improving the contribution of climate model information to decision making: the value and demands of robust decision frameworks, *WIREs Clim Change*, 4: 39–60.

Wilby, R. L., and S.Dessai (2010), Robust adaptation to climate change, *Weather*, 65(7), 180–185.

Wood, A. W., L. R. Leung, V. Sridhar, and D. P. Lettenmaier (2004), Hydrologic implications of

dynamical and statistical approaches to downscaling climate model outputs, *Climatic Change*, *62*, 189-216.

Woodhouse, C. A., S. T. Gray, and D. M. Meko (2006), Updated streamflow reconstructions for the Upper Colorado River Basin, *Water Resources Research*, *42*.

Zagona, E. A., T. J. Fulp, R. Shane, Y. Magee, and H. M. Goranflo (2001), Riverware: A generalized tool for complex reservoir system modeling, *Journal of the American Water Resources Association*, *37*, 913-929.